WINTER REGIME PERFORMANCE OF COOLING WATER DISCHARGE STRUCTURE, ZION NUCLEAR PLANT, LAKE MICHIGAN

by

J. C. Tatinclaux, S. C. Jain, J. M. Pena and J. F. Kennedy

Sponsored by

The Commonwealth Edison Company
Chicago, Illinois

IIHR Report No. 157

Iowa Institute of Hydraulic Research
The University of Iowa
Iowa City, Iowa

March, 1974

WINTER REGIME PERFORMANCE OF COOLING WATER DISCHARGE STRUCTURE, ZION NUCLEAR PLANT, LAKE MICHIGAN

by

J. C. Tatinclaux, S. C. Jain, J. M. Pena and J. F. Kennedy

Sponsored by

The Commonwealth Edison Company
Chicago, Illinois

IIHR Report No. 157

Iowa Institute of Hydraulic Research
The University of Iowa
Iowa City, Iowa

March, 1974

ABSTRACT

A thermal model study of one discharge structure of the Zion Nuclear Station on Lake Michigan was performed to investigate the behavior of the effluent plume under winter conditions. Two series of tests were carried out. The first was concerned with a deeply submerged undistorted model of the structure, the second with a distorted model in which the ratio of depth of submergence to structure height was equal to the prototype ratio of four. In all the experiments the temperature of the ambient flow was kept approximately constant at 32.2°F, and that of the effluent at 52.2°F. Initial mixing of the effluent with the ambient flow appears to be greater with the distorted model than with the deeply submerged undistorted model. Several values of the ratio K of the initial jet velocity to the ambient flow velocity were also investigated. It was found that the mixing becomes independent of the ratio K, for values of K larger than 3 to 4. In all cases a sinking plume was observed to be formed, with the highest temperatures being recorded along the bottom of the experimental flume. Excess temperatures amounting to 15 percent or more of the initial temperature difference were measured at the downstream end of the experimental flume, and a similar excess in temperature above ambient temperature is to be expected near the plant discharge over an area of the bed of Lake Michigan larger under calm, winter conditions than that occupied by the summer surface plume.

ACKNOWLEDGEMENTS

This study was sponsored by the Commonwealth Edison Company, Chicago, Illinois. All of the experiments were conducted by Jose Peña, under the supervision of S.C. Jain and J.F. Kennedy. This report was prepared by J.C. Tatinclaux and J.F. Kennedy. The cooperation of the members of the Institute of Hydraulic Research workshop, who built the experimental setup, is gratefully acknowledged.

TABLE OF CONTENTS

LIST OF FIGURES

LIST OF TABLES

WINTER REGIME PERFORMANCE OF COOLING WATER DISCHARGE STRUCTURE, ZION NUCLEAR PLANT, LAKE MICHIGAN

I. INTRODUCTION

Commonwealth Edison Company's Zion nuclear power plant, which is located on the western shore of Lake Michigan in the vicinity of Zion, Ill. has two identical generating units with a combined capacity of 2,100 Mw. The station uses once-through cooling, with the cooling water withdrawn from and returned to Lake Michigan. At full plant load, the total cooling water discharge is 1,500,000 gpm (3,340 cfs) with a temperature rise of 20°F (11.1°C) across the condensers. The cooling water is intaken through a submerged structure located approximately 2,600 ft away from the shoreline, at a point where the water depth is approximately 22 ft, and discharged back into the lake through two submerged structures, each located some 760 ft from the shore and 154 ft on either side of the intake structure, at points where the water depth in the lake is approximately 12 ft. The discharge structures are positioned on the lake bottom, and each has a rectangular discharge opening with an effective width of 74 ft and a height of 3 ft. A schematic drawing of the cooling water intake and discharge system is given in Fig. 1. Further details of the intake and discharge structures are given in the reports presenting results of experimental (Lantz and Lisauskas 1971) and theoretical (Pritchard 1971a, b) studies of the system.

After construction of the cooling system was completed, concern arose for the behavior of the plumes of heated effluent under winter conditions, when the temperature of the water in the lake is close to 32°F. As shown in Fig. 2, the density of the water reaches a maximum at a temperature of 4°C (39.2°F), and has the same value for temperatures of 0°C (32°F) and 8.1°C (46.6°F). Therefore, when water with temperatures above 8.1°C is released into a body of water with temperature near 0°C, the plume trajectory will rise to the point along its length where the plume temperature is reduced, by mixing with and entrainment of surrounding colder water, to 8.1°C. Thereafter, the density of the plume water is larger than that of the surrounding fluid, the buoyancy is negative, and the plume sinks. If this reversal in the plume buoyancy occurs before the plume reaches the free surface of the lake, little cooling of the effluent is achieved by heat transfer to the atmosphere. Instead, there is the possibility that the effluent will spread over the lake bottom as a density current, with the heat transfer then taking place to and through the overlying colder water, and the lake bed will be exposed to higher than normal temperatures, over an area which would be of the same order of magnitude as the summer surface plume.

To gain an improved understanding of the mechanics of sinking plumes, an analytical and laboratory study was undertaken at the Iowa Institute of Hydraulic Research. The analytical phase of the study is reported by Peña and Jain (1974) and the results of the experiments on round jets are given in Peña's thesis (1974). This report represents the results of the laboratory study of an idealized model of one of the Zion Station discharge structures.

II. MODELING CONSIDERATIONS

The dimensionless parameters relevant to the flow considered in the present investigation are:

1. The jet Reynolds number, $\mathbb{R} = V_j D/\nu$, where V_j is the jet velocity; $D = 4R_h$, with R_h the hydraulic radius of the slot; and ν is the kinematic viscosity of the effluent.

2. The jet densimetric Froude number, $\mathbb{F}_D = V_j/\sqrt{\Delta\rho/\rho \; gh_j}$, where h_j is the slot height; g the acceleration of gravity; and $\Delta\rho/\rho = (\rho_j - \rho_a)/\rho_a$ is the density ratio, with ρ_j and ρ_a the densities of the jet effluent and ambient fluid, respectively.

3. The ratio h_j/d of jet height, h_j, to water depth, d.

4. The aspect ratio of the slot, w_j/h_j, where w_j is the slot width.

5. The velocity ratio, V_j/V_a, where V_a is the velocity of the surrounding water.

Each of these quantities should have the same values in the model and in the prototype. However, it is not possible strictly to satisfy both the Reynolds and Froude criteria in a model. But since, for fully turbulent flow the distribution of velocity and temperature in the plume are nearly independent of Reynolds number, provided it is sufficiently large, it suffices to adjust the flow conditions in the model such that the model Reynolds number be above the critical value for turbulent flow

$$\mathbb{R}_m = (V_j D/\nu)_m > 600 \text{ (approximately)} \qquad (1)$$

In some of the experiments, the jet Reynolds number was slightly less than this value; nevertheless, introduction of dye into the jet indicated visually that the flow was turbulent.

The density ratio, $\Delta\rho/\rho$, in the model was adjusted to take on the same value as in the prototype. The Froude law then requires simply that the model and prototype have the same conventional Froude number,

$$(V_j/\sqrt{gh_j})_m = (V_j/\sqrt{gh_j})_p \qquad (2)$$

where the subscripts m and p refer to model and prototype, respectively.

If λ_x is the length scaling law of the model, the corresponding scaling factor for the velocity and discharge are given by the Froude law of similitude, Eq. 2, as, respectively,

$$\lambda_V = \lambda_X^{1/2} \qquad (3)$$

$$\lambda_Q = \lambda_x^{5/2} \qquad (4)$$

As will be discussed in Section IV, geometric similarity and the Froude criteria could not always be satisfied simultaneously because of limitations imposed by the experimental facility. Other steps then had to be taken to make the results be relevant to the prototype situation.

III. EXPERIMENTAL APPARATUS AND PROCEDURES

The experiments were conducted in the Low Temperature Flow Facility of the Iowa Institute of Hydraulic Research. The overall experimental system, a schematic diagram of which is given in Fig. 3, is composed of a variable temperature water supply system, a recirculating flume, and a temperature measuring system.

A. Variable Temperature Water Supply System. The water supply system, which is located outide of the Low Temperature Flow Facility Room, is depicted in Fig. 4. Water withdrawn from the laboratory constant head tank (CHT) is pumped through four gas-fired heaters connected in series and into the hot water line (HWL). The discharge through the cold water line (CWL) is provided by water pumped from a tank containing water at 32.2°F (CWT). These two water lines merge to form the input water line (IWL), which is insulated to prevent temperature variation by heat transfer to the surroundings. In each of these lines the flow rate is controlled by valves. Further, in order to allow for a wide range of discharges, the input water line is divided into two parallel branches, one equipped with a one-eighth-inch orifice meter for low discharges, the other with a three-eighth-inch orifice meter for measurement of higher discharges. The temperature of the water in the input line was monitored with a precision thermometer located immediately upstream from the branching point.

In the present experiments, the discharges modeled were extremely low, being only a few thousandths of one cubic foot per second at the most. It was necessary, therefore, to incorporate two waste water lines (WW1 and WW2) into the system, in order to control the flow accurately. These waste water lines were also used to purge the water supply system of any air bubbles which might have been present.

B. Recirculating Flume. The experimental flume is 40 ft long, 2 ft wide, and 1 ft deep. The circulating water in the flume is propelled by a variable speed pump, and the flow rate was measured either by a Venturi meter for high discharges or by an orifice meter for lower discharges. The sidewalls and bottom of the flume were fabricated from special refrigeration plates through which a temperature controlled ethylene glycol solution is circulated, thereby providing temperature regulation of all or parts of the flume boundary. However, during most of the experiments, the heated water discharged through the slot raised the temperature of the water circulating in the flume to such a degree that the cooling provided by the downstream portion of the walls and the bottom of the flume proved inadequate for restoring the initial upstream ambient temperature. Supplementary cooling was then provided by filling the downstream sump tank of the flume with crushed ice, and installing near the downstream end of the flume a battery of cooling tubes through which coolant was circulated.

C. Temperature Measurement System. The temperature measuring system consisted of 10 to 14 probes fabricated from thermistors made of a semi-conductor with negative temperature-resistance coefficient of about $0.04/^{\circ}C$, which is approximately ten times larger than that of normal conductor metals. One probe was positioned upstream from the slot and used to measure T_a, the initial ambient temperature; a second was placed in the feed line to the slot and measured T_j, the effluent temperature; and the other probes were placed at various positions in the downstream flow field to measure temperatures from which the plume configurations were determined. The probes were mounted on a specially designed carriage and could be shifted easily from one position to another. Each probe was interfaced through its own bridge circuit with the Institute's IBM 1800 Data Acquisition and Control System. The sensors were calibrated at about fifteen temperatures between $0^{\circ}C$ and $22^{\circ}C$, and the calibration relations so obtained were quantified by a least-squares fit to a second-order polynomial and stored in computer memory. The calibrations were checked prior to every run in order to detect and correct either any faulty sensor or any variation in the calibration curves. The outputs from the thermistor bridges for each position setting of the probes were fed directly to the computer, which averaged the voltage outputs over a period of 60 seconds or longer, and then printed out for each probe the average voltage, the corresponding temperature calculated from the probe's calibration curve, and the normalized temperature difference, $(T - T_a)/(T_j - T_a)$. The temperature measurements are judged to be accurate to

$\pm 0.05^{\circ}C$. The corresponding accuracy in the normalized temperature difference is about three percent.

D. Experimental Procedure. After filling the flume at the desired depth with water chilled to $32.2^{\circ}F$, the speed of the circulating water pump was adjusted to give the required discharge and velocity in the working section of the flume. When a jet is discharged into a laterally unbounded, quiescent body of water, such as Lake Michigan, surrounding water is entrained into and mixed with the discharged water. This entrainment is a consequence of the exchange of momentum between the plume and the receiving fluid, and is the mechanism by which the plume fluid becomes diluted. In the experimental flume, the presence of the lateral walls restricted the supply of diluting water which could be entrained into the plume. To compensate for this restriction, an artificial current was simulated by recirculating the water in the flume. This provided a source of diluting water to be entrained by the plume. The desired velocity and temperature of the jet were obtained by trial and error by adjusting the flows in the hot and cold water lines. This tedious procedure often required several hours before steady state conditions were reached. During the establishment of the required conditions, the jet was diverted through a flexible hose into a drain. When steady state conditions were obtained, the slot was set on the bottom of the flume and its orientation was checked, by injecting dye in the nozzle, and corrected if necessary. The injection of dye also permitted verification that the flow was turbulent.

During the course of an experiment, the temperature of the jet and that of the ambient water upstream from the slot were regularly monitored. If the ambient temperature increased by more than $1.2^{\circ}F$, the run was discontinued until acceptable conditions were reestablished. Temperature distributions were measured at four to eight cross-sections downstream from the nozzle in each run. The vertical and lateral spacings of the measurement points were adjusted as needed to obtain adequate definition of the plume geometry.

IV. SUMMARY OF EXPERIMENTS

The discharge structure of each unit of Zion Station consists of a slot 75 ft wide and 3 ft high. At its location the lake is approximately 12 ft deep, yielding a submergence ratio of 4. The temperature difference across the condenser is 20°F. The discharge through the structure is 1,670 cfs, with a corresponding efflux velocity of 7.42 fps. The corresponding value of the conventional Froude number is 0.755, and that of the densimetric Froude number is 62 for winter-regime conditions.

Two series of experiments were performed. In order to gain some insight in the mechanics of sinking plumes, the first series was conducted using an undistorted, deeply submerged model of the discharge structure, so that the effect of the free surface would be negligible. In the second series of experiments, the submergence ratio, d/h_j, had the same value in the model as in the prototype, but for reasons spelled out later, geometric similarity could not be achieved and a distorted model had to be used. In all tests the temperature difference between the receiving water and the slot discharge was maintained at 20°F, the prototype value, and therefore, the density ratio in the model was the same as in the prototype.

A. Undistorted Model. The height of the model was chosen to be 3/32 in, with a corresponding width of 2-11/32 in. The Froude criterion of similitude then yields a jet velocity of 0.38 fps, and a corresponding discharge of $5.78\ 10^{-4}$ cfs. The heat input into the flume in this case was sufficiently small that it could be removed through the flume boundaries by the circulating coolant, and the ratio of slot width to flume width was large enough for the blockage effect to be negligible. The model jet Reynolds number was, however, only 422, somewhat below the critical value of 600. Injection of dye indicated that the jet was nevertheless turbulent. The depth of submergence was kept constant at 0.9 ft in all the runs of this series, corresponding to a ratio d/h_j of 115. A total of four runs were conducted under these conditions for four different values of the velocity ratio $K = V_j/V_a$. The experimental conditions are summarized in Table 1.

B. Distorted Model. The rate of heat removal from the circulating water was limited by the cooling capacity of the walls and bottom of the downstream portion of the flume, even after additional cooling was supplied by filling the downstream sump of the flume with crushed ice and placing in the flume a battery of cooling coils through which coolant was circulated. Since the temperature of the jet was imposed to be 20°F higher than that of the ambient water, the limitation in heat input produced a limitation on the jet discharge. The maximum jet discharge then possible led to a minimum value of the discharge scaling factor λ_Q of about 560,000, which, from Eq. 4, corresponds to a length scaling factor λ_x of about 200. On the other hand, a minimum flow depth of approximately 0.2 ft had to be maintained in the flume in order to be able to control the flow with reasonable accuracy, and also to obtain temperature measurements at a sufficient number of points in a cross section to have an accurate description of the plume. Since the water depth in the prototype is 12 ft, the corresponding maximum value of λ_x is thus 60. To circumvent this impasse, it was then decided to resort to a distorted model in which the submergence ratio d/h_j would take the same value as in the prototype (i.e. $d/h_j = 4$), and the scaled discharge and jet momentum flux would be maintained, but geometric similarity of the slot and consequently the Froude law would not be respected.

The slot discharge in the model was chosen to be equal to $Q_m = 2.2\ 10^{-3}$ cfs, corresponding to $\lambda_Q = 7.59\ 10^5$ and $\lambda_x = 225$; the resulting heat input to the flume was sufficiently small that the required ambient temperature could be maintained. The corresponding jet velocity in the model was $V_m = 0.493$ fps. The depth of flow in the flume was chosen to be 2.25 inches. Therefore, in order to have the same value of d/h_j in the model and in the prototype ($d/h_j = 4$) the height of the slot was fixed at 9/16 in. The width of the slot which produced the required jet velocity and discharge was $w_m = 1\ 5/32$ in. The corresponding value of the densimetric Froude number in the model was $\mathbb{F}_D = 22$ as compared to a value of 62 in the prototype. Both of these values were judged to be sufficiently large that the mixing was practically independent of $\mathbb{F}_D$. The jet Reynolds number in the model was $R_e = 2,500$, well in the turbulent range.

Five runs were performed under these conditions for five different values of the velocity ratio K, ranging from 1 to 10. The experimental conditions for this series of tests are summarized in Table 2.

IV. RESULTS AND DISCUSSION

The experimental results are presented in Figs. 5 to 8, in which the number shown at each point gives the ratio of excess temperature above ambient temperature $(T - T_a)$, to the difference between jet temperature and ambient temperature, $(T_j - T_a)$, in percent. The temperature distribution at various cross sections downstream from the discharge plane are given in Figs. 5a to 5d for the deeply submerged undistorted model, and in Figs. 7a to 7e for the distorted model. The temperature distributions along the centerplane of the flume are presented in Figs. 6a to 6d for the undistorted model, and in Figs. 8a to 8e for the distorted model.

From this latter set of figures (Figs. 6 and 8), it can be seen that, because of the large initial mixing and the initial increase of density with temperature, the plume trajectories (defined as the locus of the maximum temperature at each section) do not rise; instead, at every section the largest temperature occurs at or near the bed. A similar situation was observed in the field study of the discharge plumes from the Waukegan Station on Lake Michigan under calm winter conditions, as reported by Pipes, Pritchard, and Beer (1973).

A. Effect of free surface. By comparing the temperature distributions in the plumes for the deeply submerged jet and for the shallow jet for an identical value of K (see Figs. 5a, 6a, and 7d, 8d, respectively, for K = 5, or Figs. 5b, 6b, and 7e, 8e, respectively, for K = 10), it appears that the proximity of the free surface tends to enhance the mixing of the jet with the surrounding water, since at comparable distances from the discharge structure the plume temperatures are always larger for the case of the deeply submerged, undistorted model, than for the case of the distorted model in shallow water. In Fig. 6a and 8d, for example, it is seen that the 30, 20, or 15 percent isotherms extend approximately four to five times farther downstream in the former case than in the latter one. However, it should be recalled that the jet Reynolds number for the shallow case was much larger than for the deep case, 2500 and 422 respectively, and that consequently the corresponding difference in the jets' turbulence structure may be responsible for part of the difference in the intensity of mixing of the effluent with the surrounding water.

B. Effect of K. The effect of the velocity ratio, K, can be evaluated qualitatively by comparing the isotherms in Figs. 8a to 8e for the jet in shallow water, to which the present discussion will be limited. When the velocity ratio V_j/V_a is increased from 1 to 3.2 (Figs. 8a and 8b, respectively), the temperature distribution at any section downstream from the discharge plane shows an increase in the temperature in the plume, and the downstream extent of the plume, as measured by the center plane lengths of the 20 percent and 30 percent isotherms, is increased by a factor of 2, approximately. Comparison of Figs. 7a and 7b indicates that the plume also widens as K increases. The overall effect is an increase of the areas contained within the same isolines. This indicates a decrease in the dilution of the effluent by entrainment of and mixing with the receiving water. Further increase in the velocity ratio K appears to have little effect on the mixing of the effluent with the surrounding water, as is evidenced by the almost idential pattern of the isotherms shown in Figs. 8c to 8e, and by the similar temperature distributions presented in Figs. 7c to 7e.

C. Plume behavior. This discussion will be limited to the case of the jet in shallow water, which represents more closely the field situation at Zion Station. From the temperature distributions measured for different K's at x/h_j = 11, the closest section to the discharge structure where measurements were obtained, it can be seen that the initial intense mixing of the effluent with the receiving water creates a relatively narrow column of warm water, of density larger than that of the surrounding fluid. As this column moves downstream, it sinks and spread laterally over the bed of the flume, entraining and mixing with the colder surrounding layers of fluid. A similar situtaion was studied experimentally and semi-analytically by Prych (1970), who released a "slot" of denser fluid in a current. His results show that the denser fluid sinks and spreads over the bottom of the flume in a manner very similar to that observed in the present situation. The maximum temperature at any section is found at the bed, while the temperature at the free surface remains nearly equal to that of the receiving water. Therefore, little if any heat transfer to the atmosphere can be expected at the free surface, and cooling of the heated effluent will be achieved primarily through mixing with and dilution by the receiving water. In the experimental flume, temperatures in excess of 3°F above the temperature of the receiving water were recorded near the bottom of the flume as far downstream from the discharge structure as it was possible to obtain measurements, and at the last section investigated, completely across the flume. No quantitative estimate of the dimensions of the inverted thermal wedge that will form in Lake Michigan can be achieved from the results of this study, since the lateral spread of the warm layer in the flume was limited by the walls; however, temperatures of the order of 3°F above ambient can be expected over an area of the lake bed comparable to the area of the summer surface plume of similar temperature rise, unless there are significant tidal or littoral currents. The field study at Waukegan Station indicates that surface distrubances induced by wind may be sufficient to prevent the formation of such a layer at the bottom of the lake, and provide a more thorough dilution by the receiving water.

V. CONCLUSION

A study of the mixing characteristics of a discharge structure of the Zion Nuclear Station under calm winter conditions has been performed. Under these conditions, where the temperature of the receiving body of water, Lake Michigan in the present case, is near the freezing point, the warm effluent spreads over the bottom of the lake, and the heat transfer will take place mainly to and through the overlying colder water, with little or no heat loss to the atmosphere, since at the free surface the temperature stays nearly equal to the ambient temperature. The temperature measurements obtained in the model study indicate that in the protoptype temperatures in excess of 3°F above ambient temperature are to be expected over some area of the lake bed, which cannot be evaluated quantitatively from experiments conducted in a relatively narrow flume as was the case in this study. Actual in sites measurements could be performed to verify and compliment the results obtained in the laboratory.

REFERENCES

1. C.H. Lantz and R.A. Lisauskas, 1971, "Zion Discharge Model Study--Zion Station, Commonwealth Edison Company of Illinois," Alden Research Laboratory Report.

2. J.M. Peña and S.C. Jain, 1974, "Numerical Analysis of Warm, Turbulent Sinking Jets Discharged into Quiescent Water of Low Temperature," IIHR Report No. 154, Iowa Institute of Hydraulic Research, The University of Iowa, Iowa City, Iowa.

3. J.M. Peña, 1974, "On the Behavior of Warm, Sinking Jets Discharged into Water of Low Temperature," M.S. Thesis, The University of Iowa, Iowa City, Iowa.

4. W.O. Pipes, D.W. Pritchard, and L.P. Beer, 1973, "Condenser Water Discharge Plumes from Waukegan Generating Station under Winter Conditions," Commonwealth Edison Company, Chicago, Illinois.

5. D.W. Pritchard, 1971a, "Predictions of the Distribution of Excess Temperature in Lake Michigan Resulting from the Discharge of Condenser Cooling Water from the Zion Nuclear Power Station," Pritchard-Carpenter Consultants Report to Commonwealth Edison Company.

6. D.W. Pritchard, 1971b, "Comparison of the Distribution of Excess Temperature as Computed Using a Numerical Prediction Model and as Observed in a Hydraulic Model of the Zion Nuclear Power Station Condenser Discharge," Pritchard-Carpenter Consultants Report to Commonwealth Edison Company.

7. E.A. Prych, 1970, "Effects of Density Differences on Lateral Mixing in Open-Channel Flows," Report No. KH-R-21, W.M. Keck Laboratory California Institute of Technology, Pasadena, California.

Table 1. Undistorted Model - Experimental Conditions

Run No.	T_j (°F)	T_a (°F)	ΔT (°F)	V_j (fps)	$100xV_a$ (fps)	K (V_j/V_a)	$\mathbb{F}_D$	$\mathbb{F}$	$\mathbb{R}_j$	$\frac{h_p}{h_m}$
U1	52.6	32.8	19.8	0.379	7.58	5	42.8	0.75	422	115
U2	52.6	32.6	20.0		3.79	10	43.0			
U3	52.8	32.9	19.9		2.2	17	41.9			
U4	52.5	32.8	19.7		1.25	30	43.4			

Table 2. Distorted Model - Experimental Conditions

Run No.	T_j (°F)	T_a (°F)	ΔT (°F)	V_j (fps)	$100xV_a$ (fps)	K (V_j/V_a)	$\mathbb{F}_D$	$\mathbb{F}$	$\mathbb{R}_j$	$\frac{h_p}{h_m}$
D1	53.0	32.2	20.8		0.493	1	21			
D2	51.0	33.3	20.7		0.153	3.2	21			
D3	52.7	33.1	19.6	0.493	0.120	4.1	22	0.40	2300	4
D4	53.8	33.3	20.5		0.0986	5	20			
D5	53.2	33.4	19.8		0.0493	10	23			

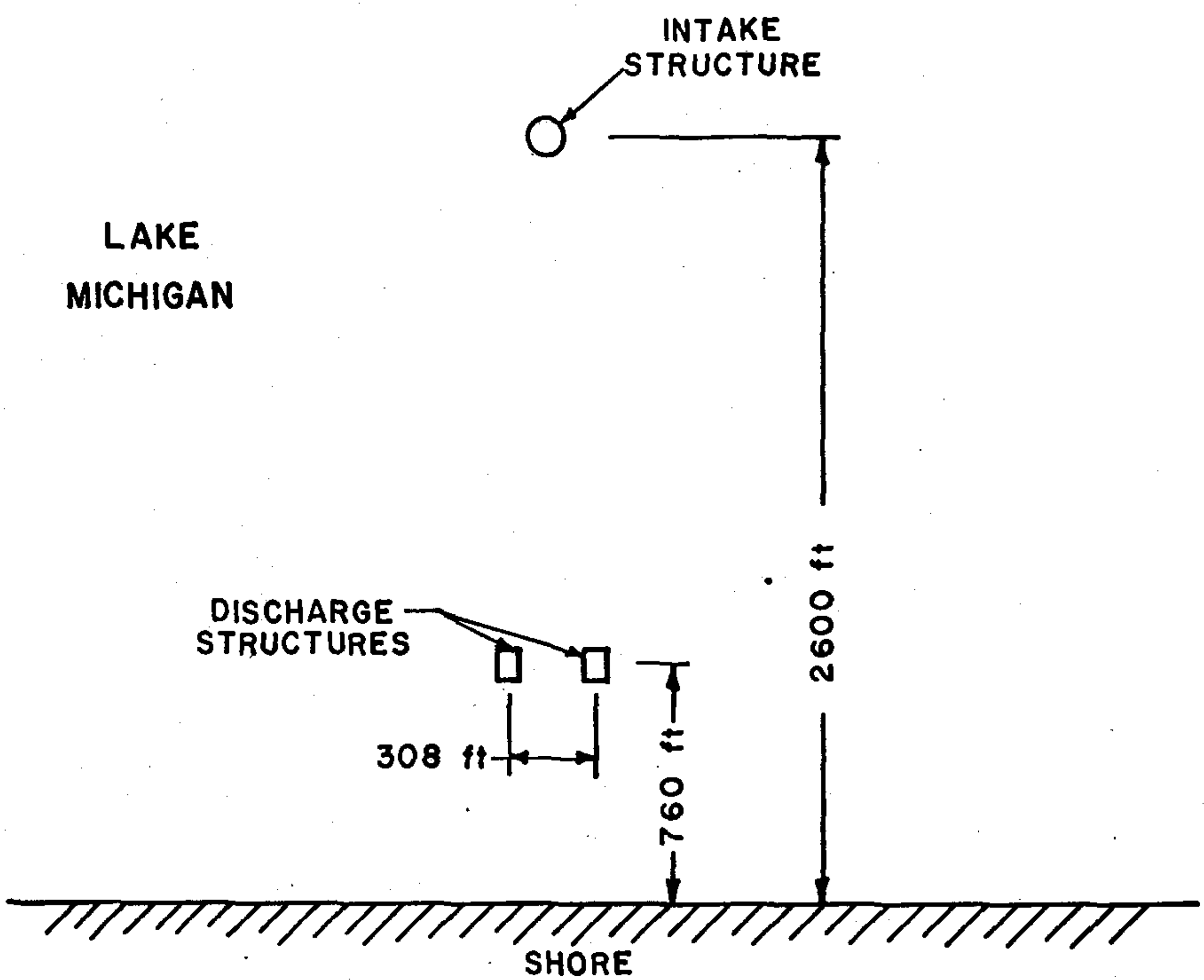

FIG. I SCHEMATIC DIAGRAM OF ZION STATION

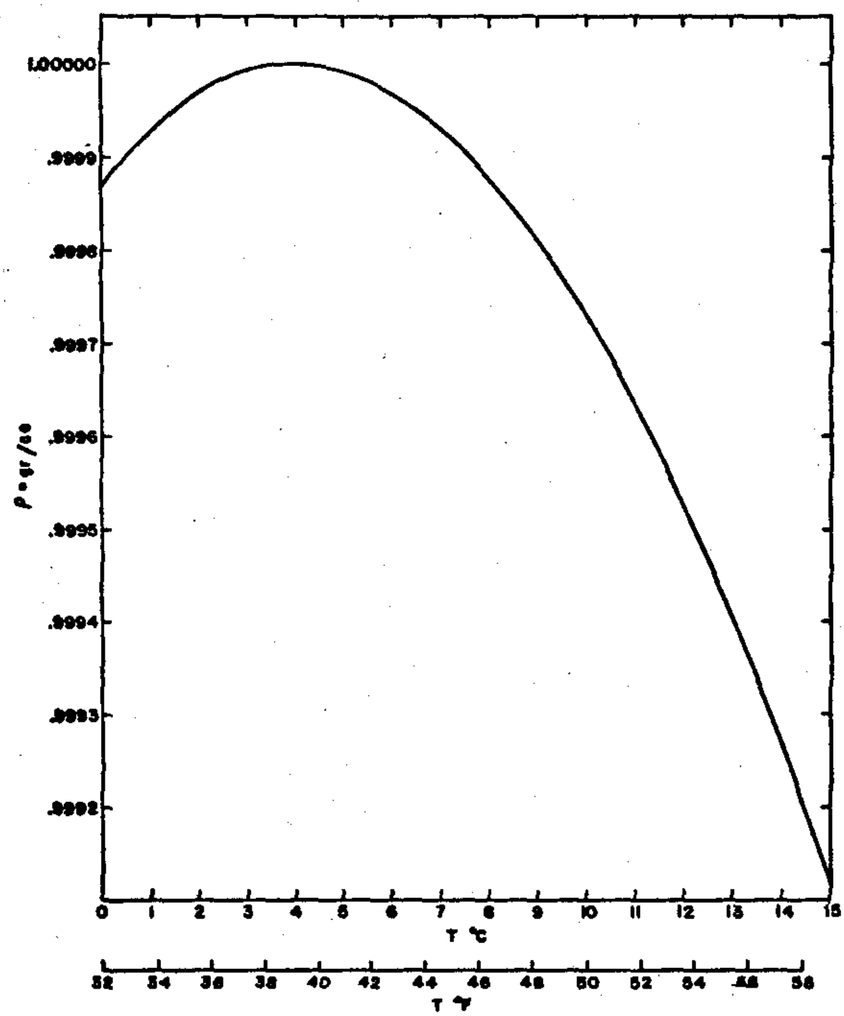

Figure 2 Water Density versus Temperature

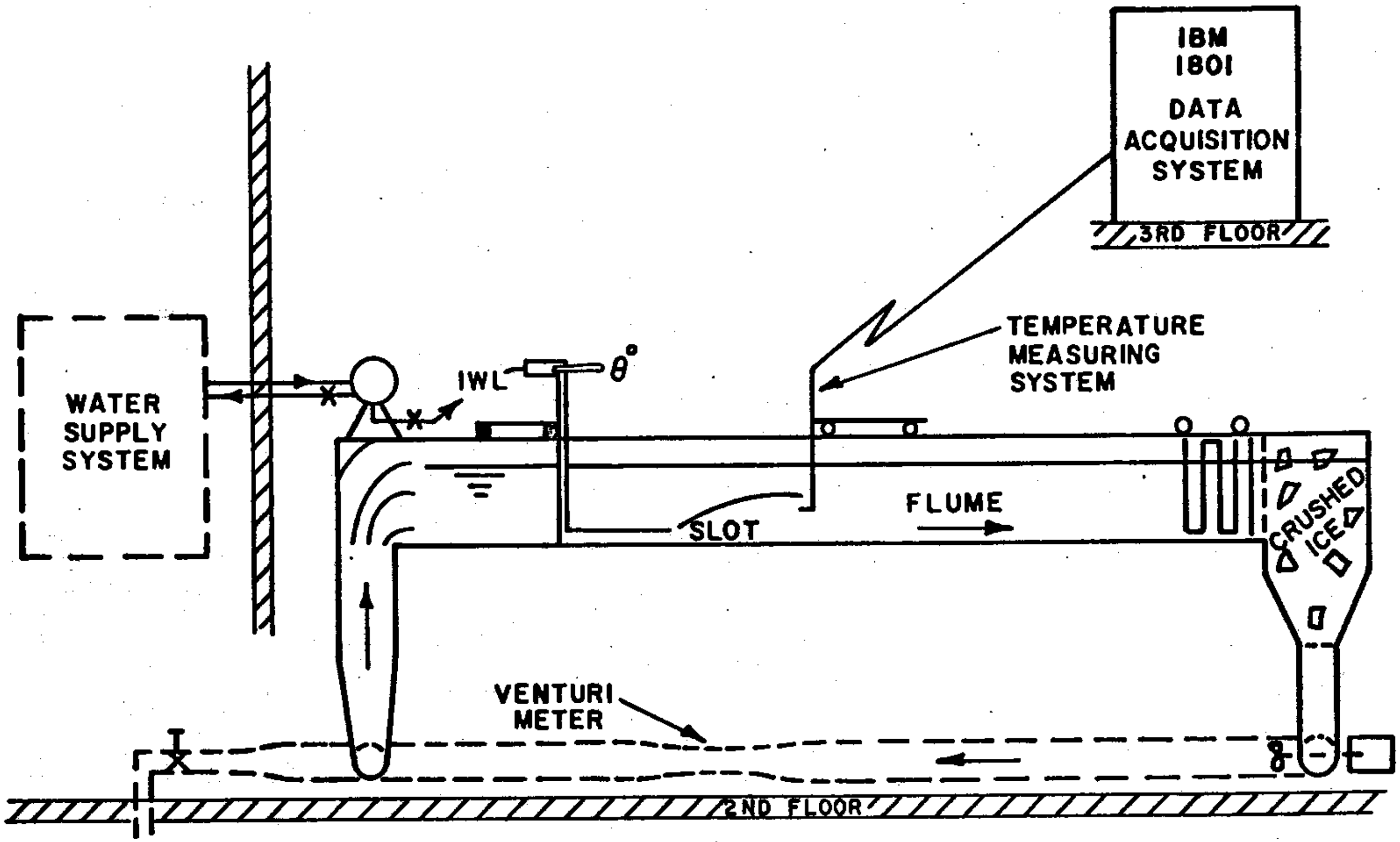

Figure 3 Schematic Diagram of Experimental Set-up

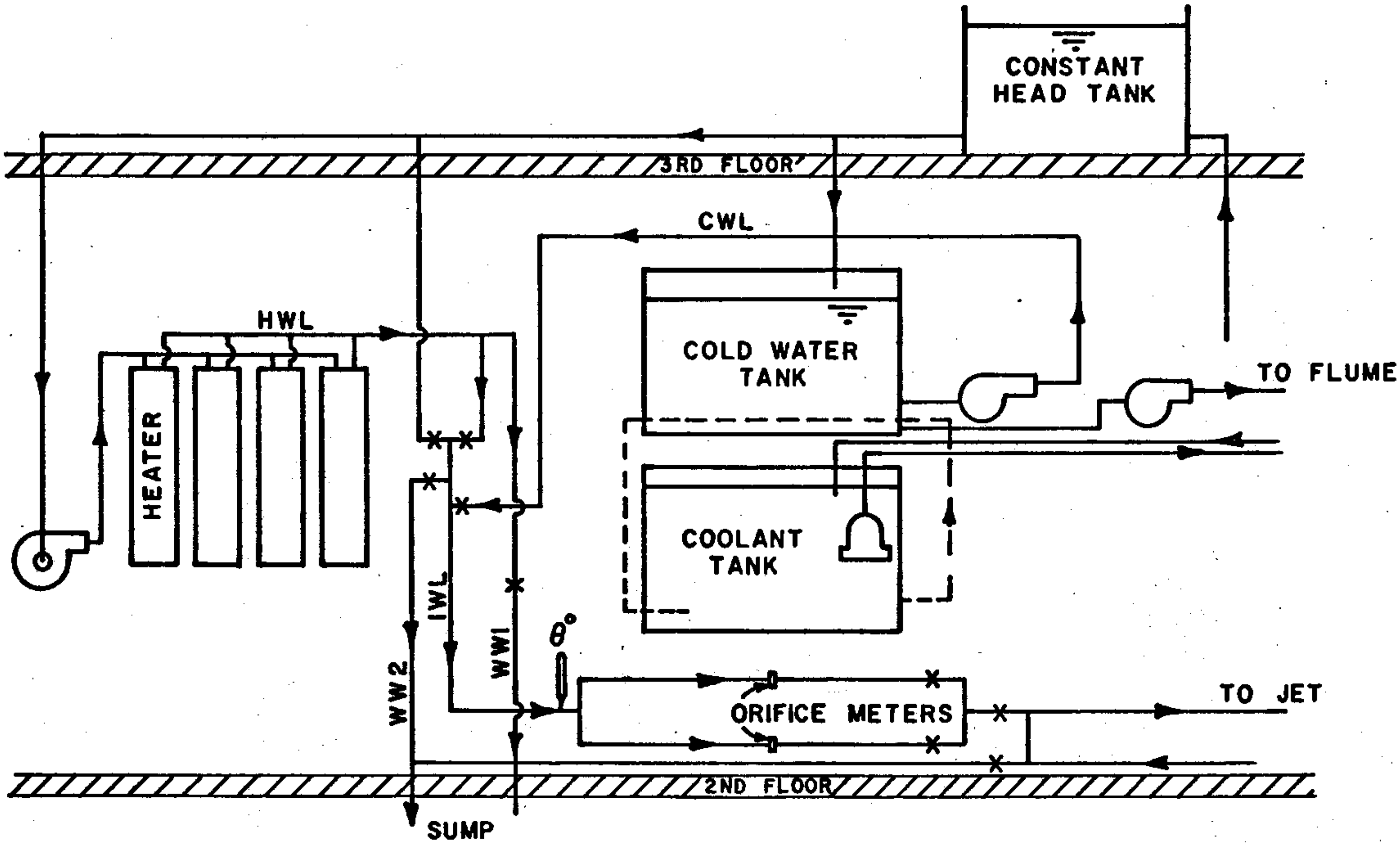

Figure 4 Schematic Diagram of the Water Supply System

Figure 5 Transverse Temperature Distributions - Undistorted Model

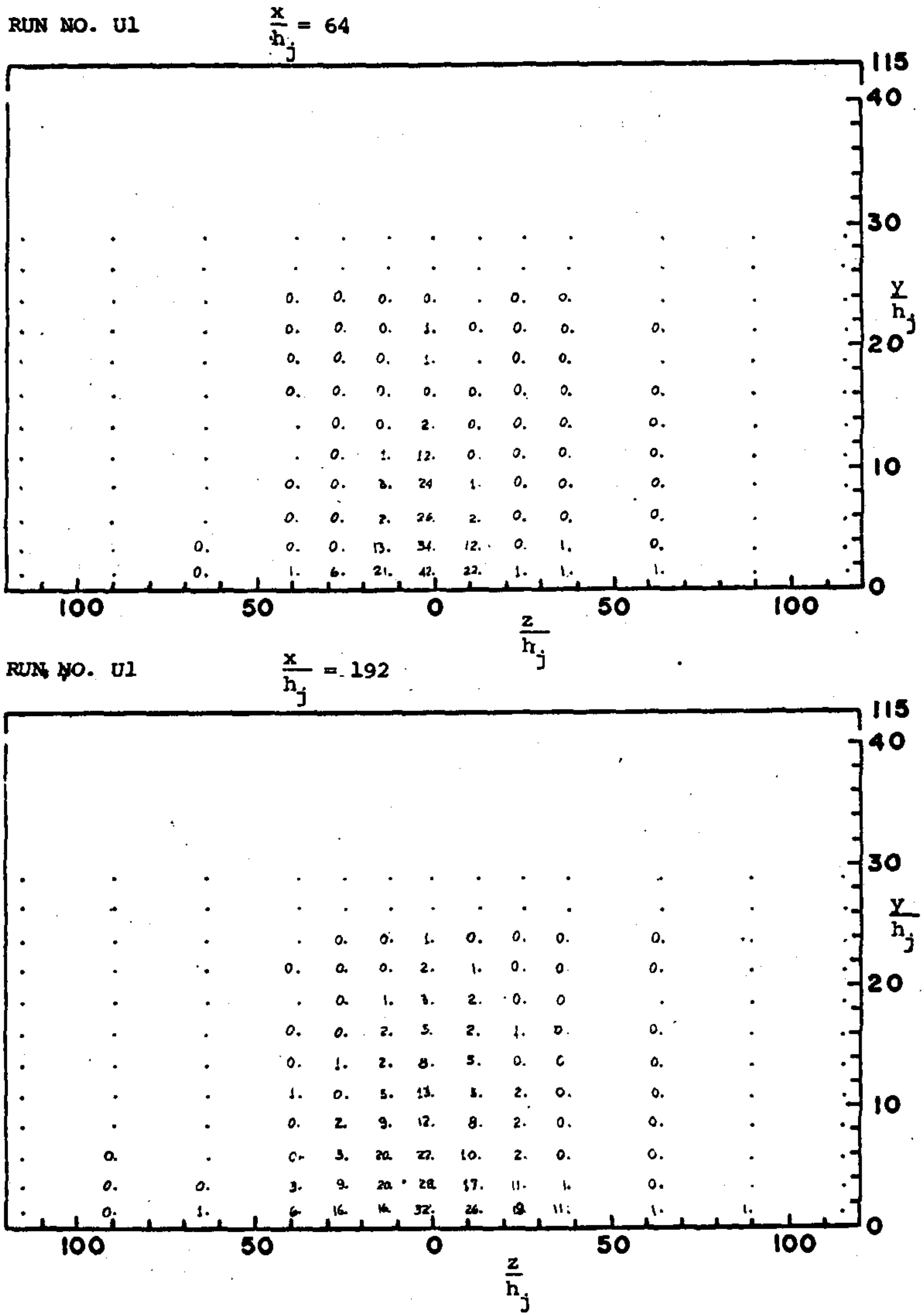
RUN NO. U1
x/hj = 64
115
40
30
20
10
0
y/hj
100
50
0
50
100
z/hj
RUN NO. U1
x/hj = 192
115
40
30
20
10
0
y/hj
100
50
0
50
100
z/hj

Figure 5a K = 5

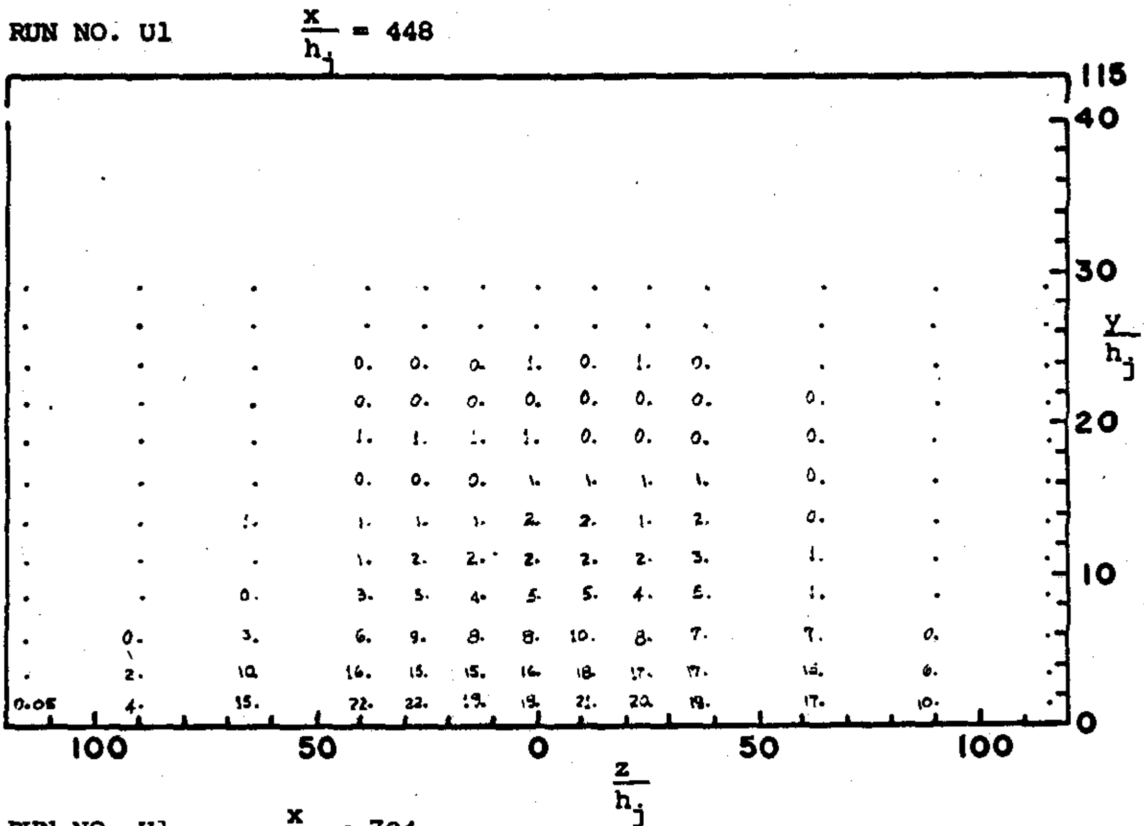

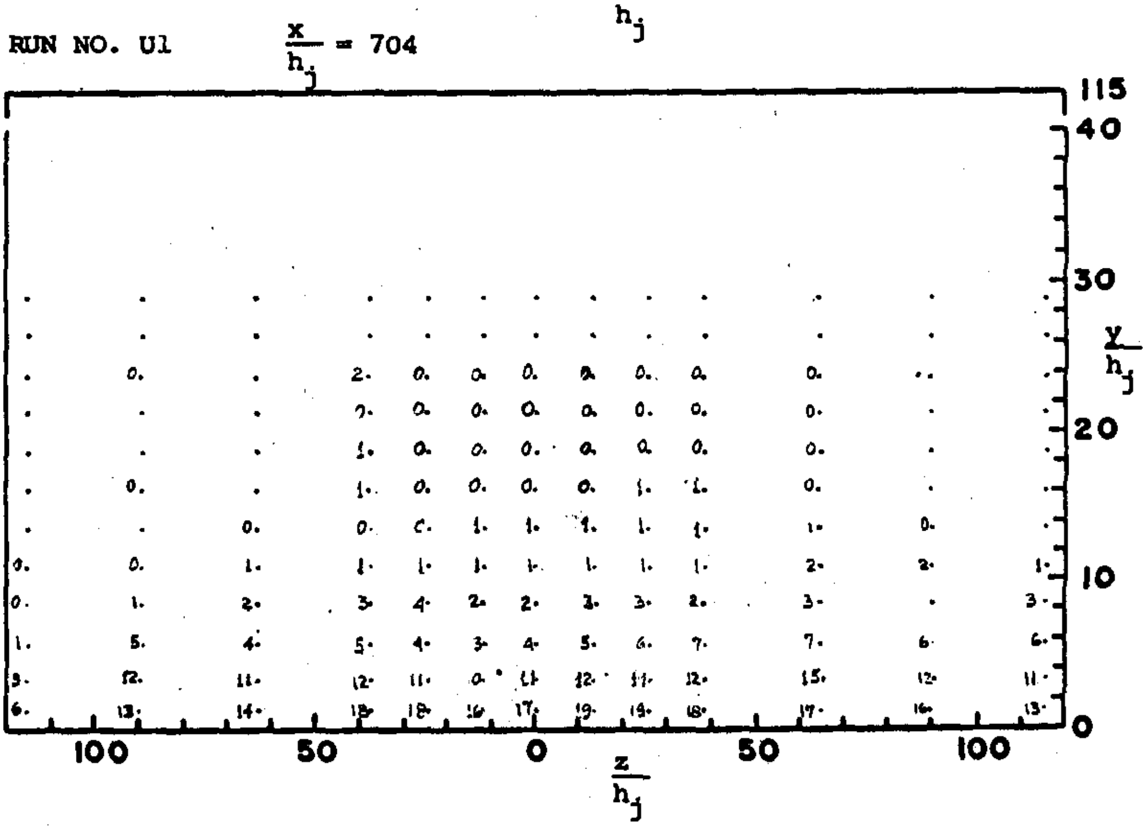

Figure 5a (ctd) K = 5

RUN NO. U1 $\frac{x}{h_j} = 960$

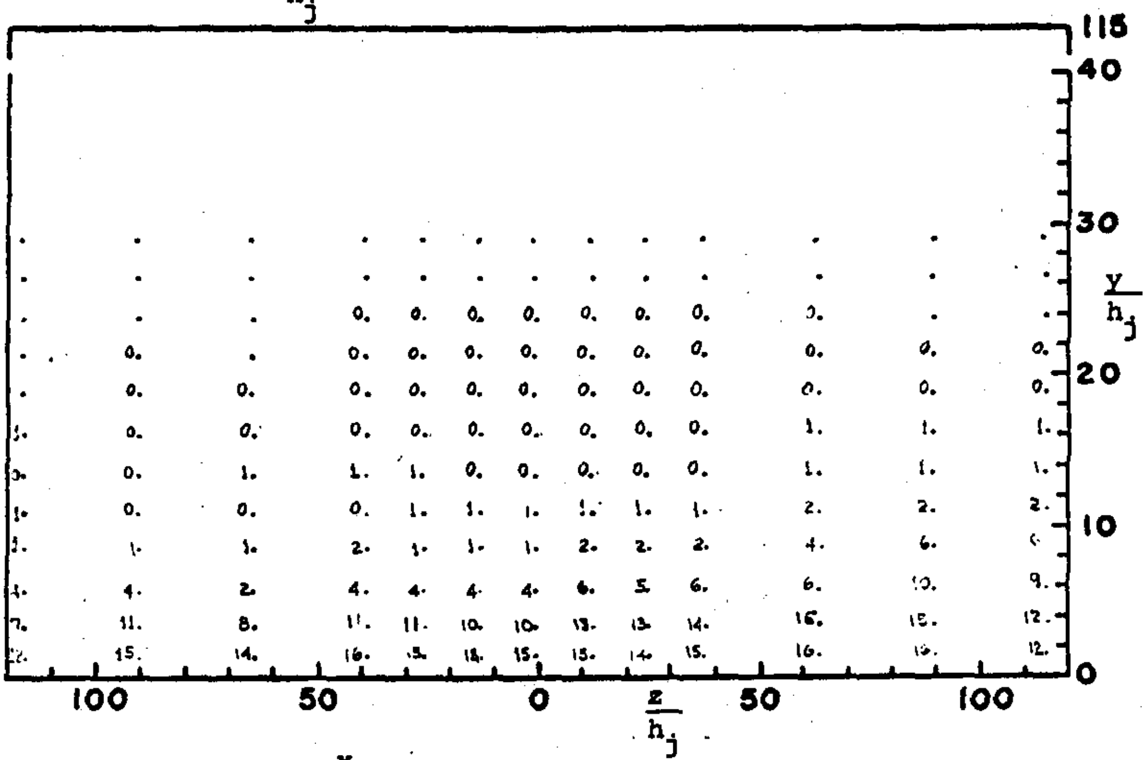

RUN NO. U1 $\frac{x}{h_j} = 1472$

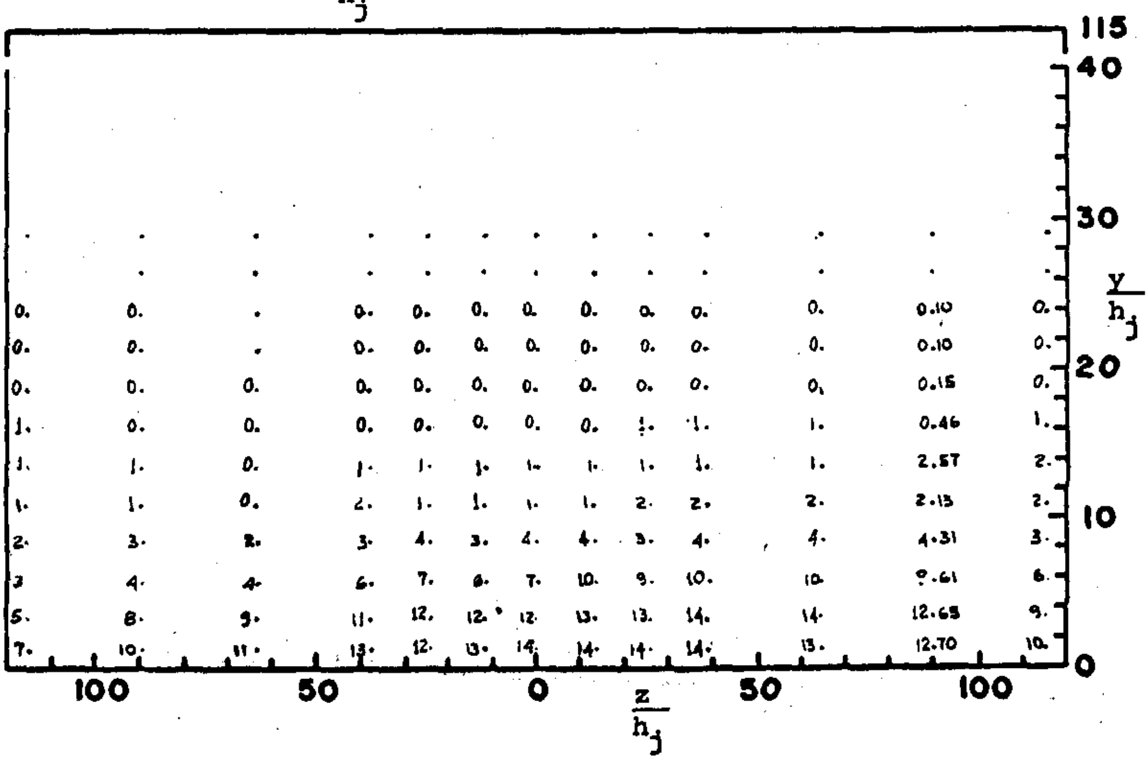

Figure 5a (ctd.) K = 5

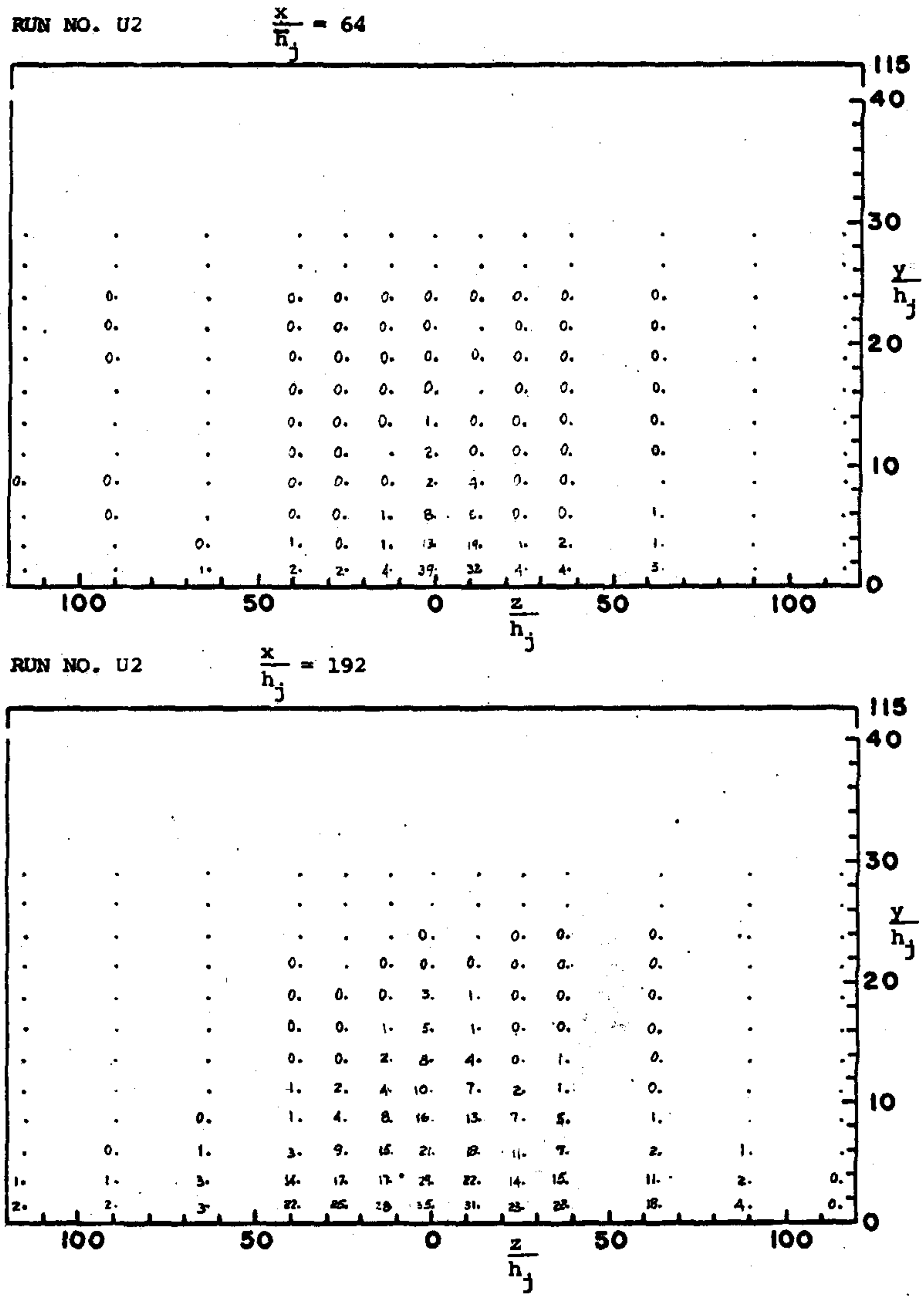

Figure 5b K'= 10

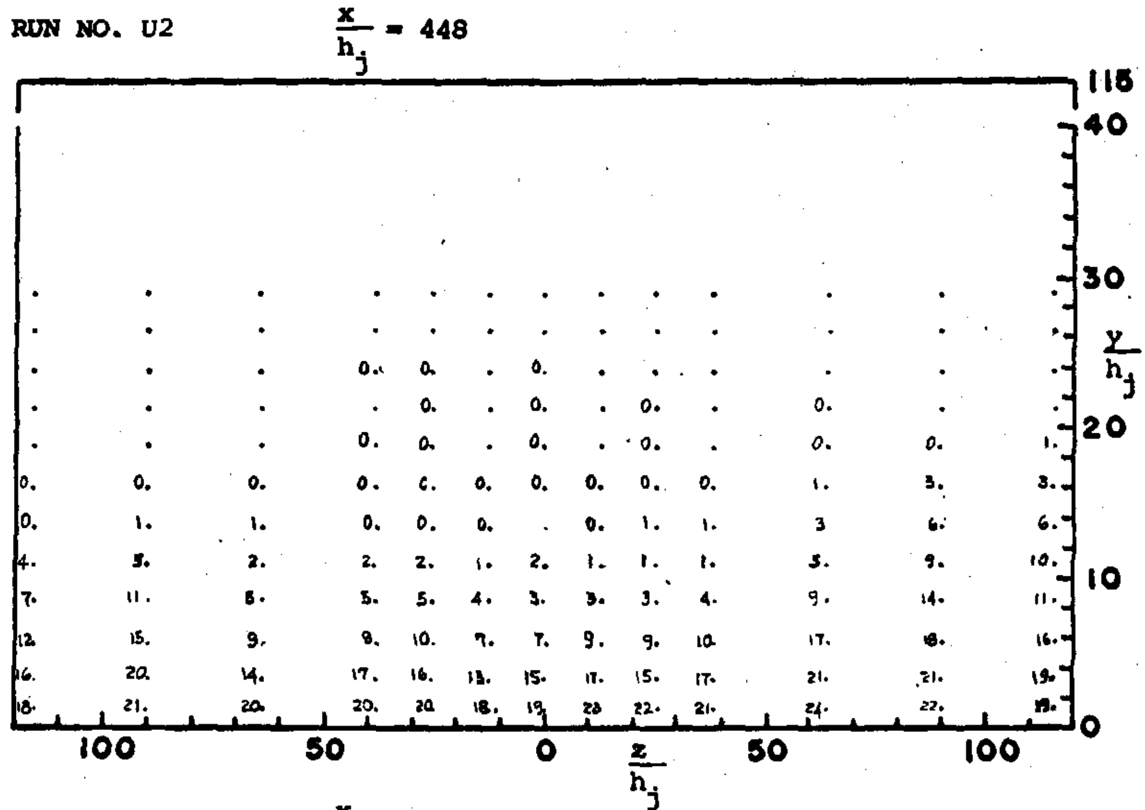

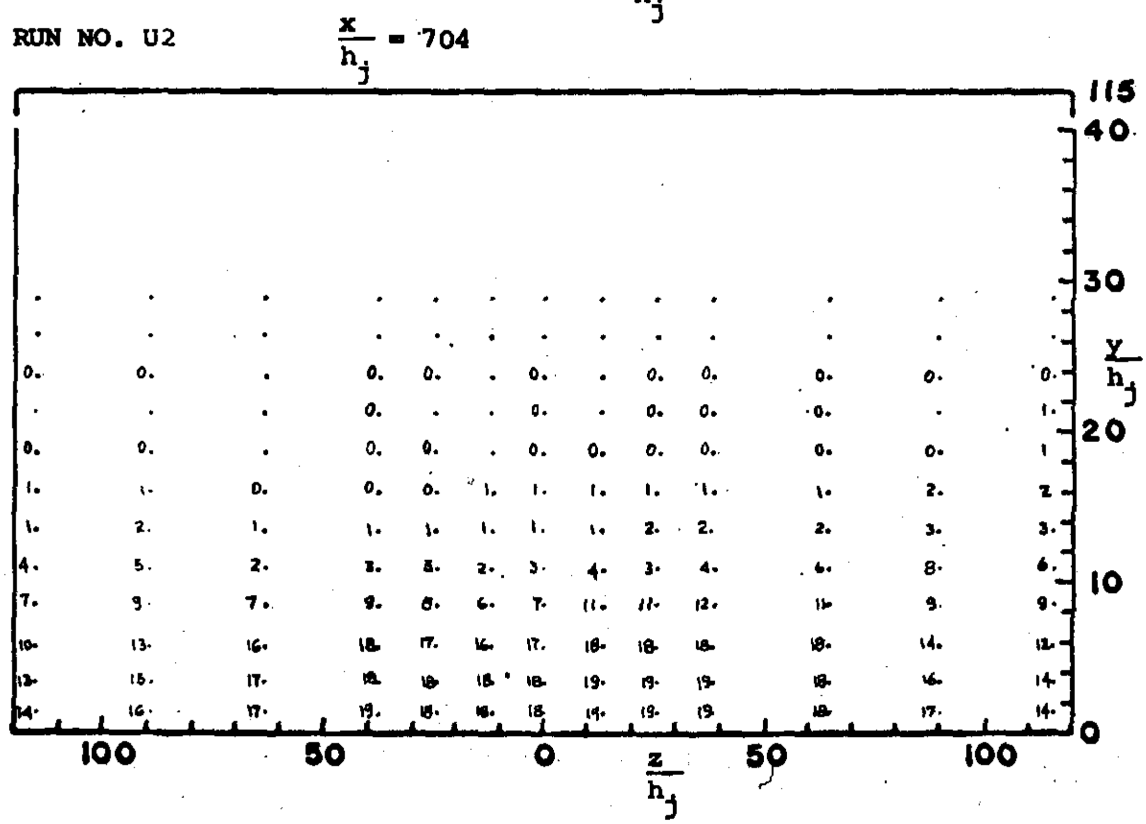

Figure 5b (ctd.) K = 10

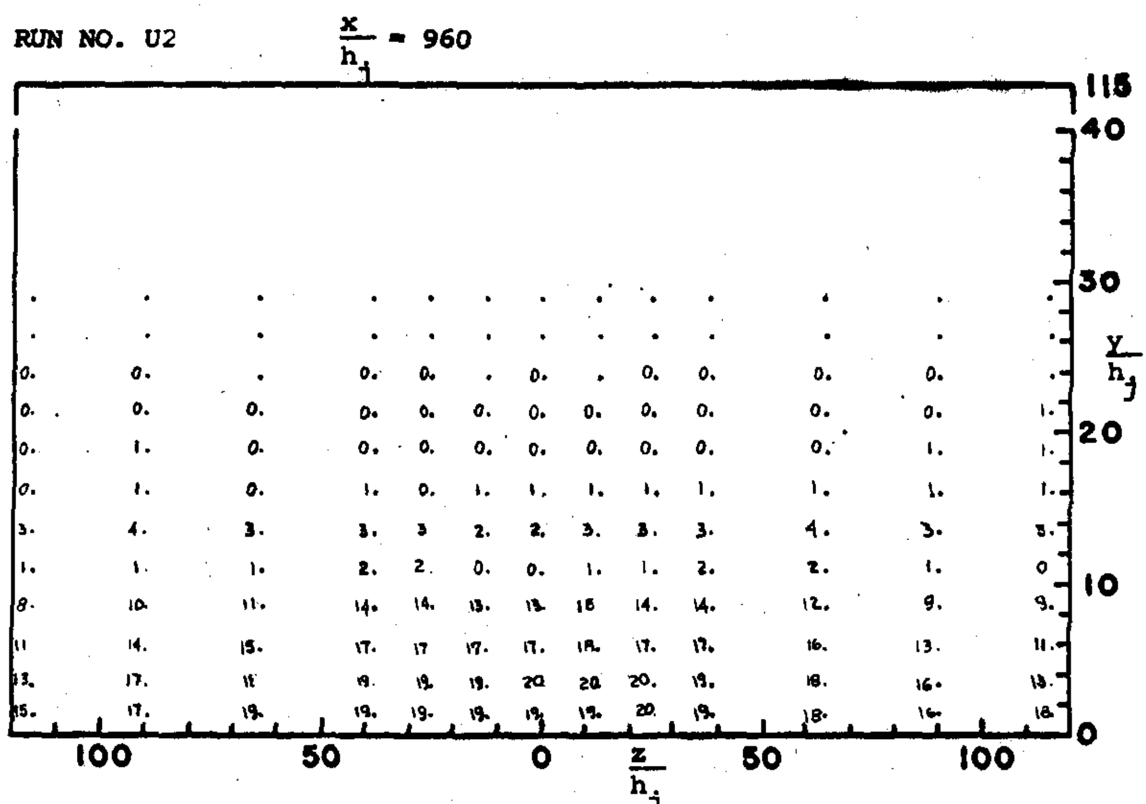

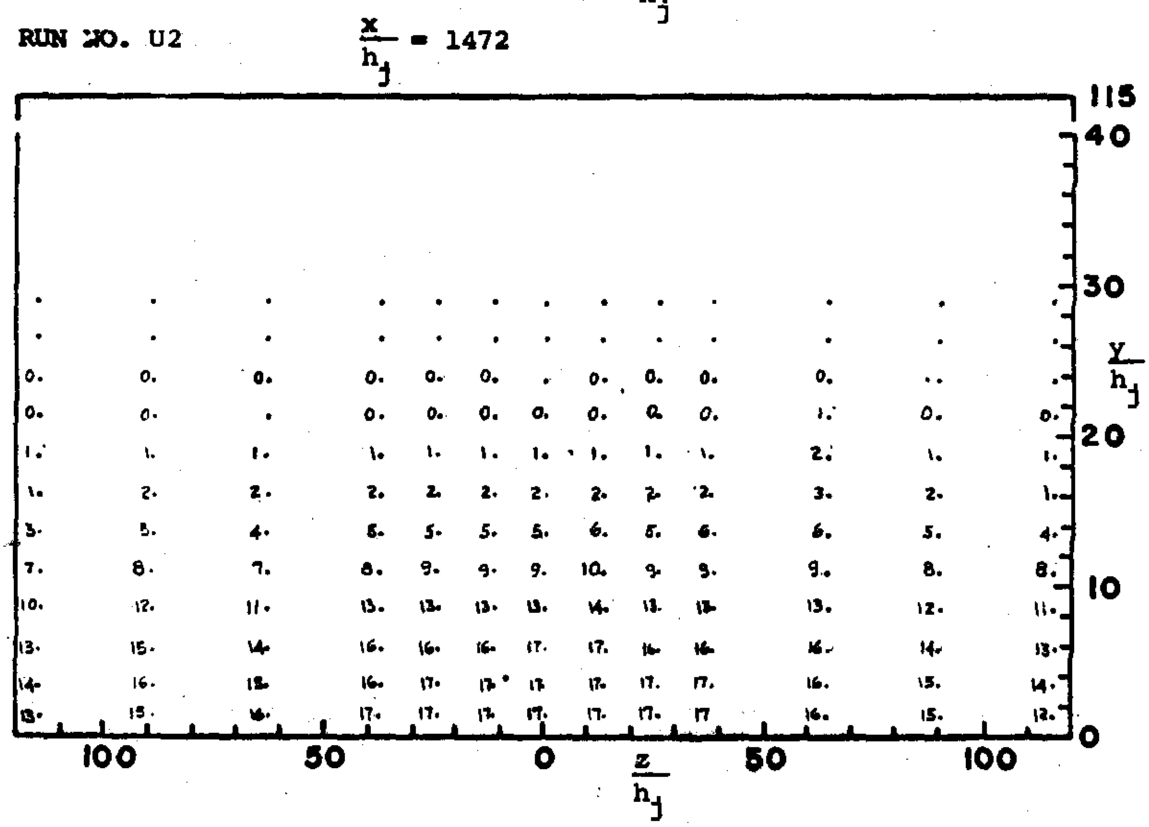

Figure 5b (ctd): K = 10

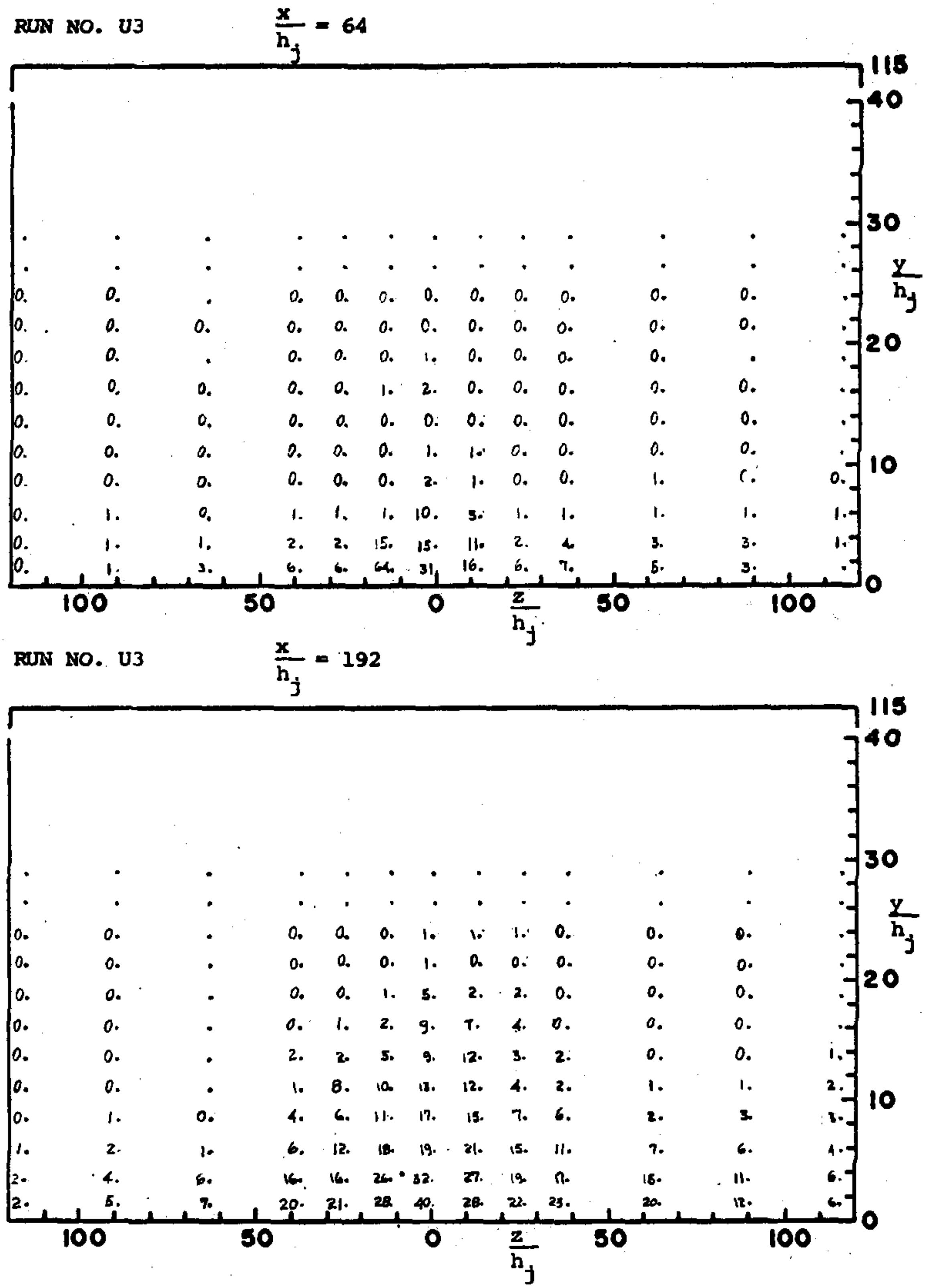

Figure 5c: K = 17

RUN NO. U3 $\frac{x}{h_j} = 448$

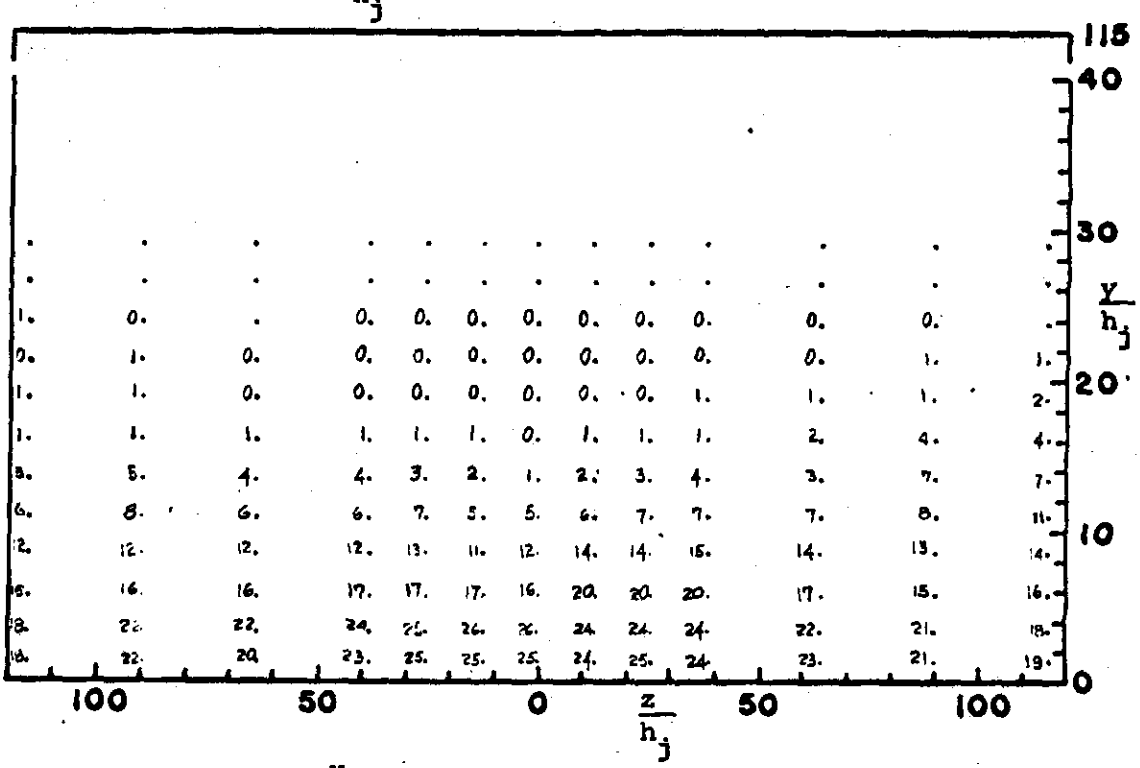

RUN NO. U3 $\frac{x}{h_j} = 704$

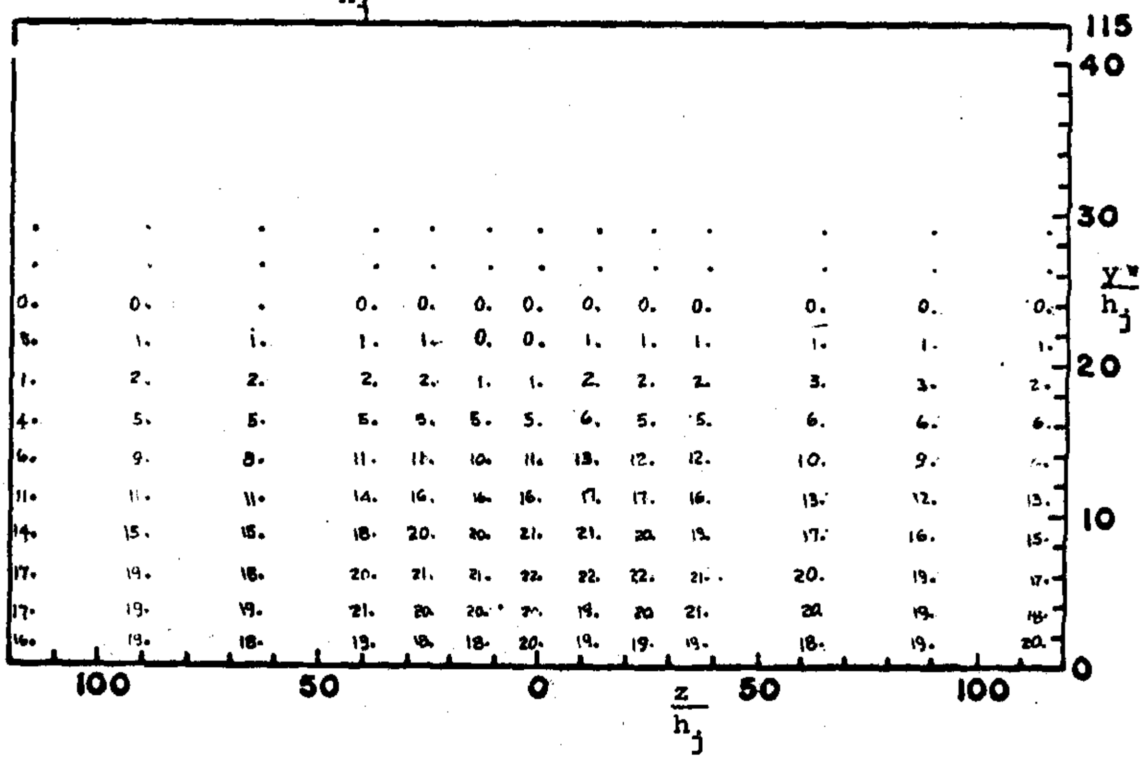

Figure 5c (ctd): K = 17

RUN NO. U3 $\frac{x}{h_j} = 960$

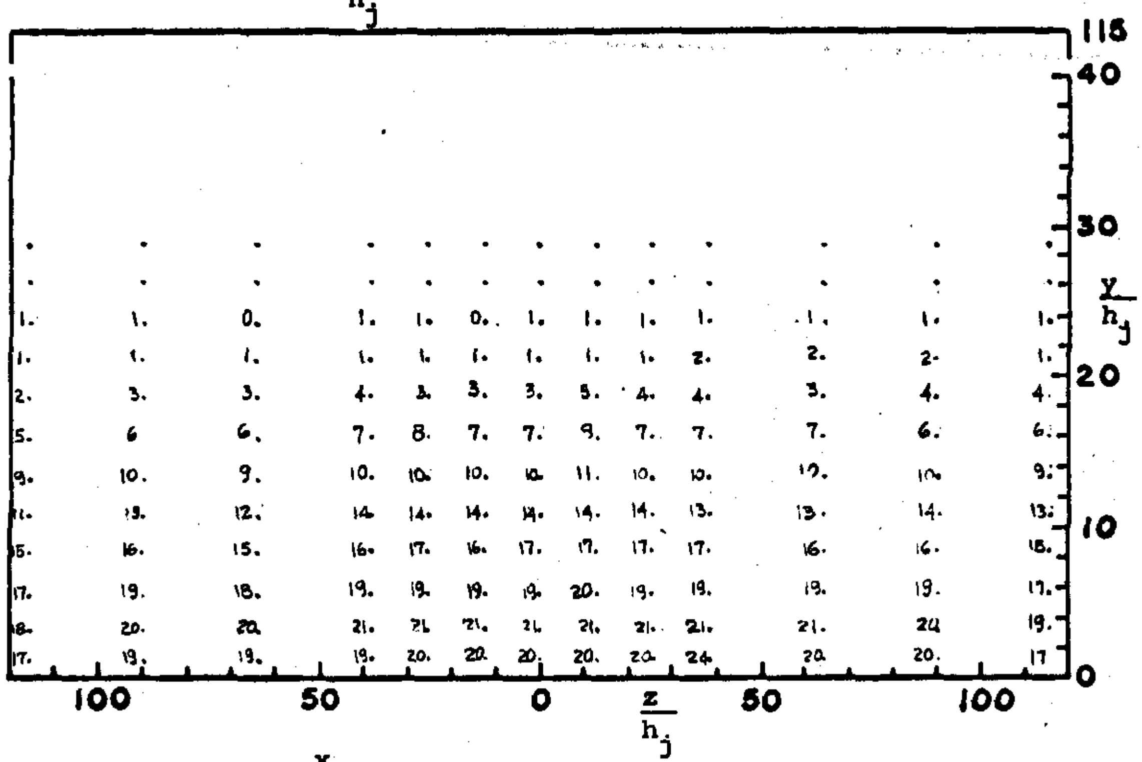

RUN NO. U3 $\frac{x}{h_j} = 1472$

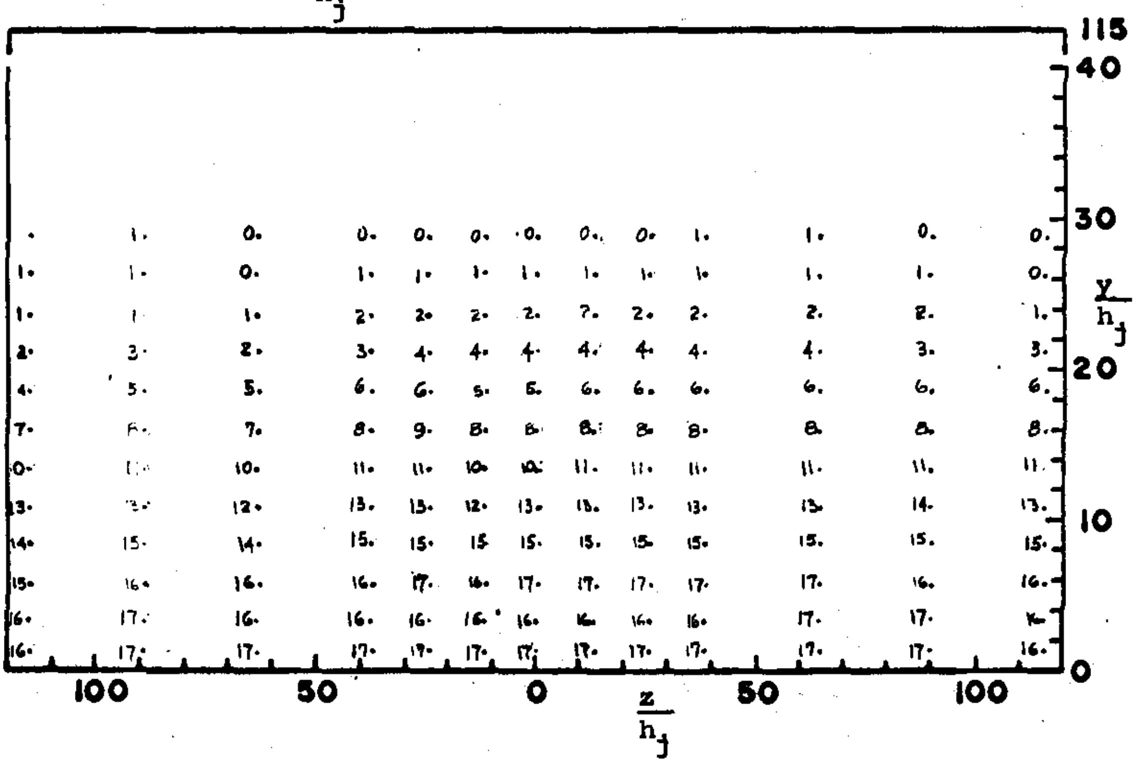

Figure 5c (ctd): K = 17

RUN NO. U4 $\frac{x}{h_j} = 64$

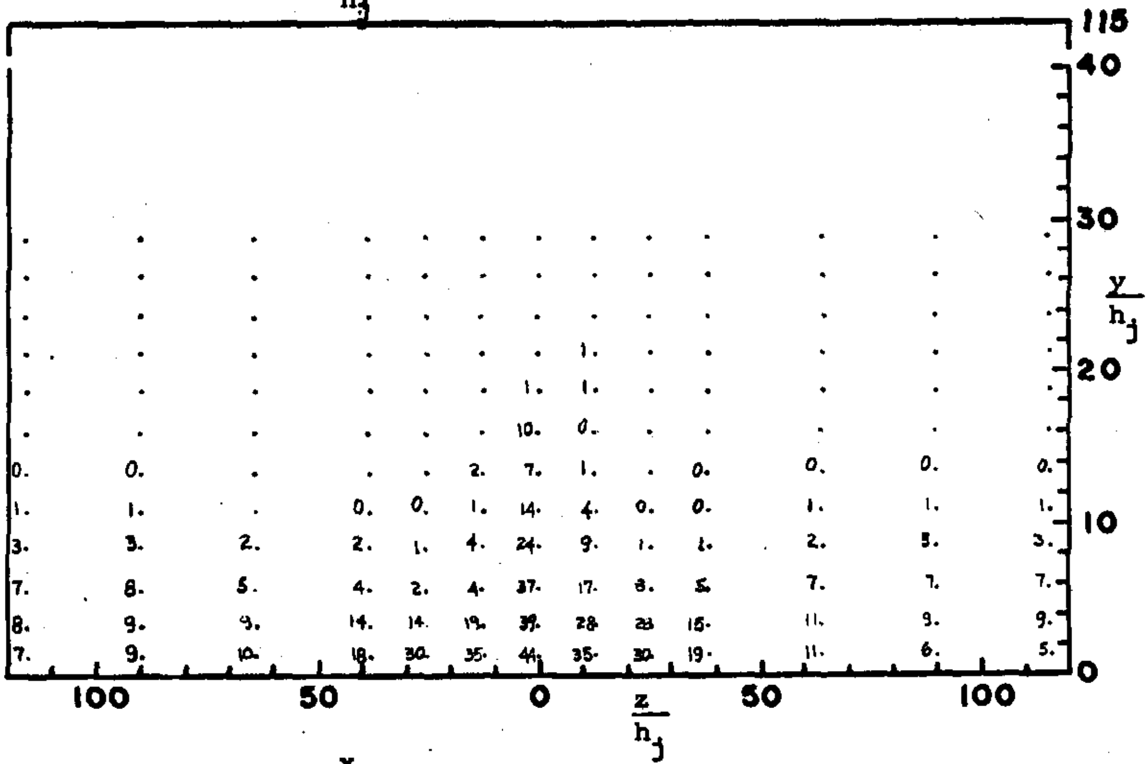

RUN NO. U4 $\frac{x}{h_j} = 192$

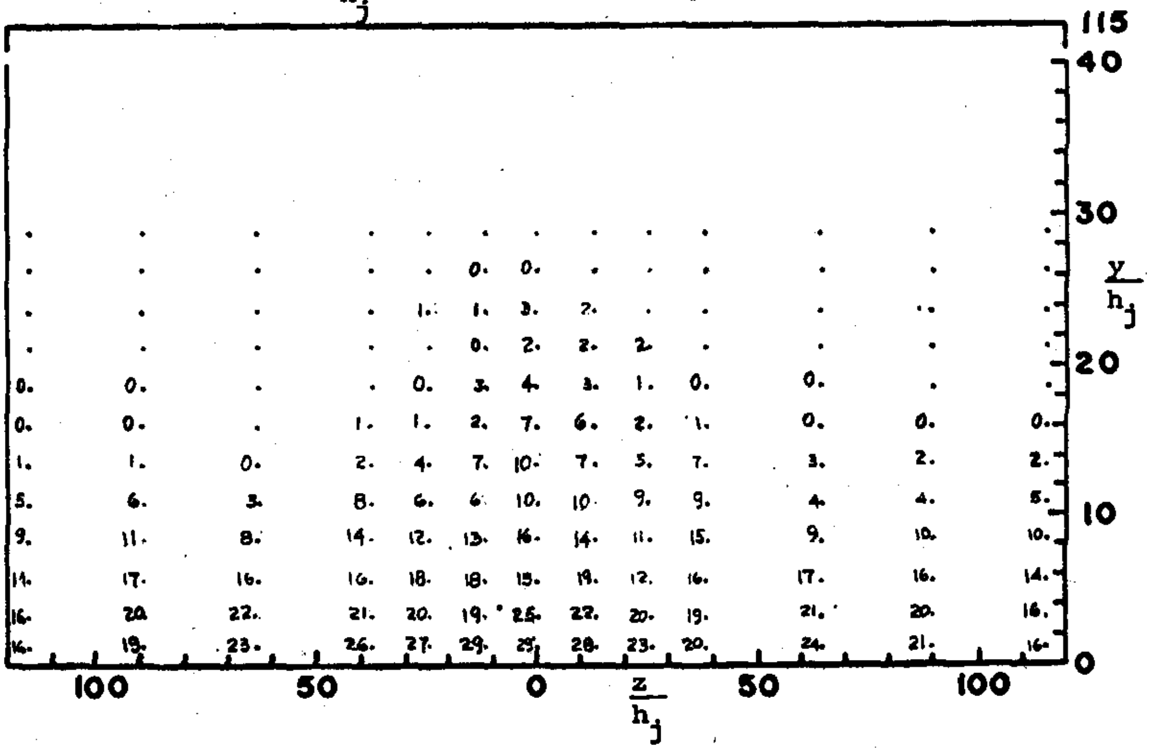

Figure 5d: K = 30

RUN NO. U4 $\frac{x}{h_j} = 448$

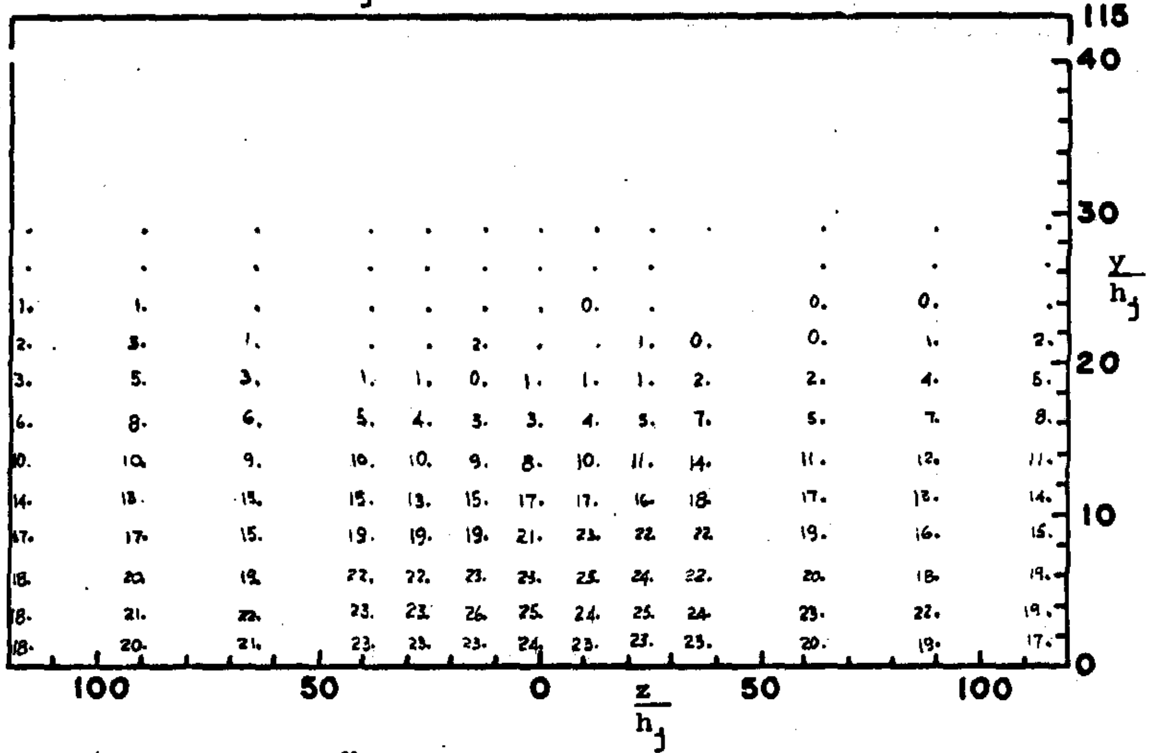

RUN NO. U4 $\frac{x}{h_j} = 704$

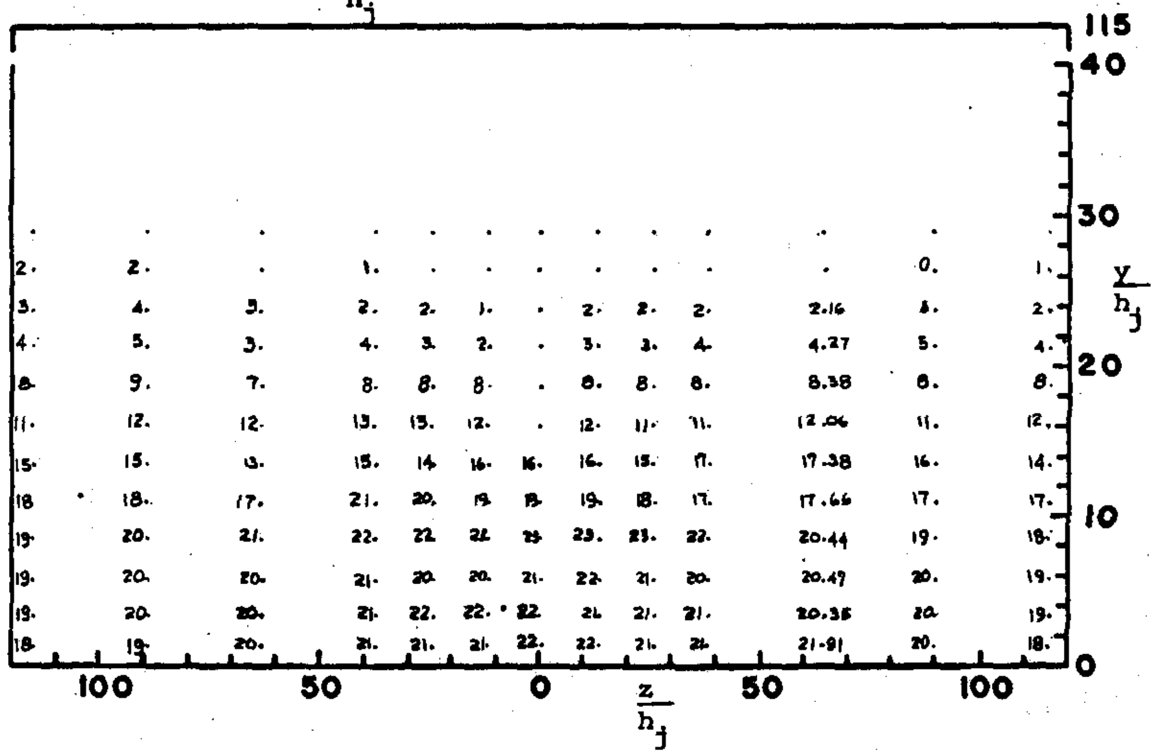

Figure 5d (ctd.) K = 30

Figure 6 Longitudinal Temperature Distribution - Undistorted Model

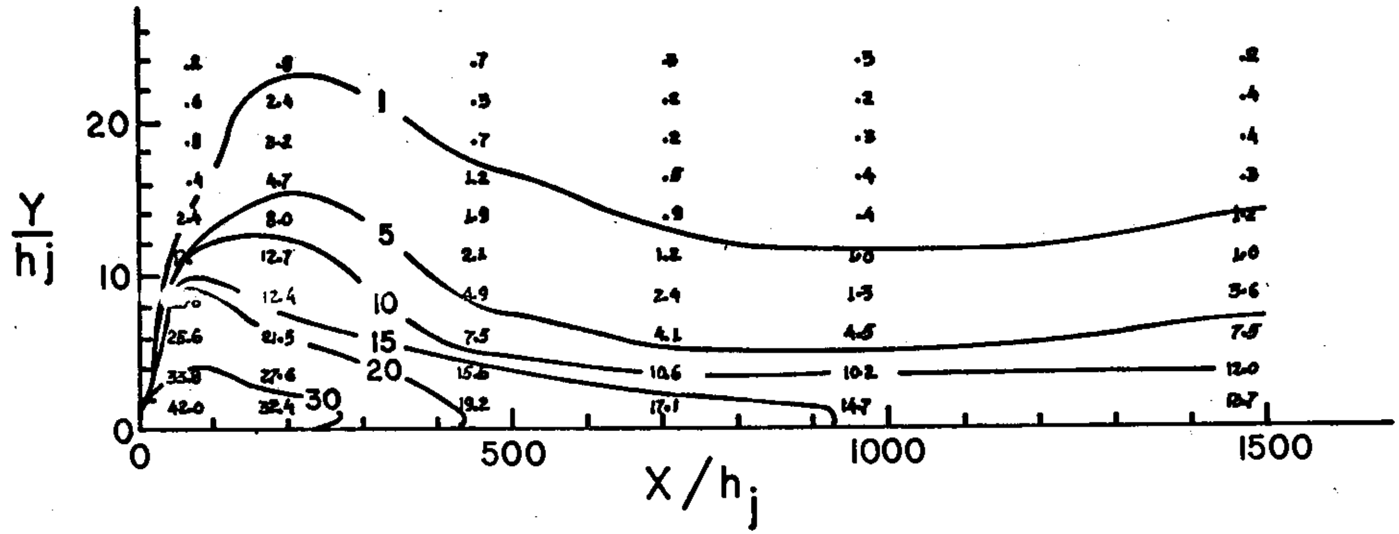

Figure 6a Undistorted Model K = 5

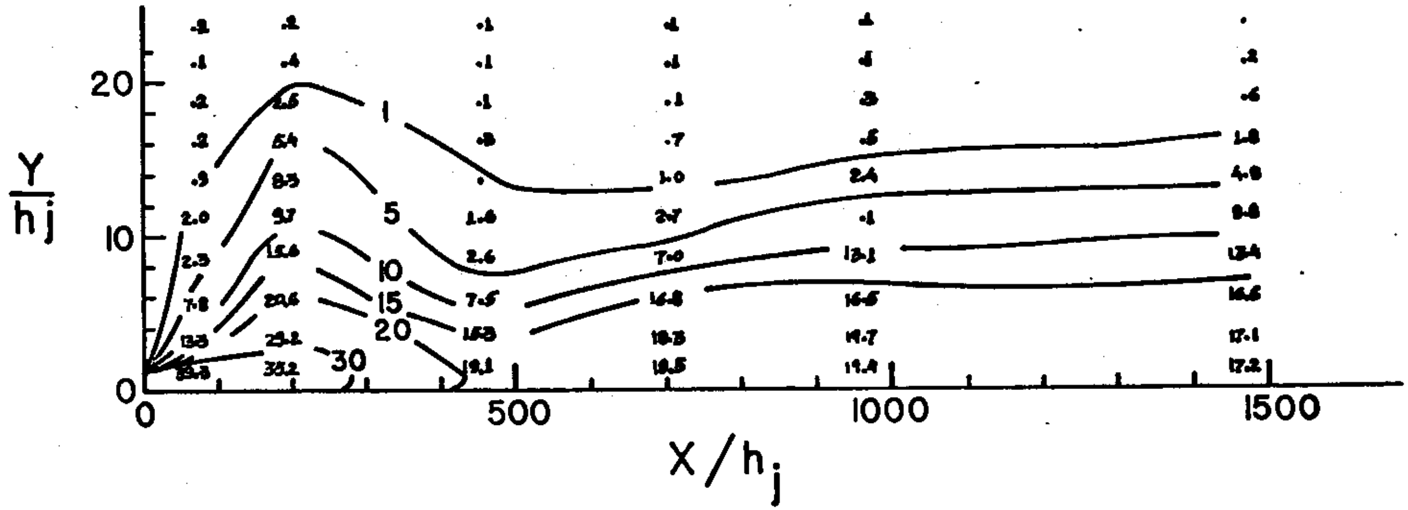

Figure 6b Undistorted Model K = 10

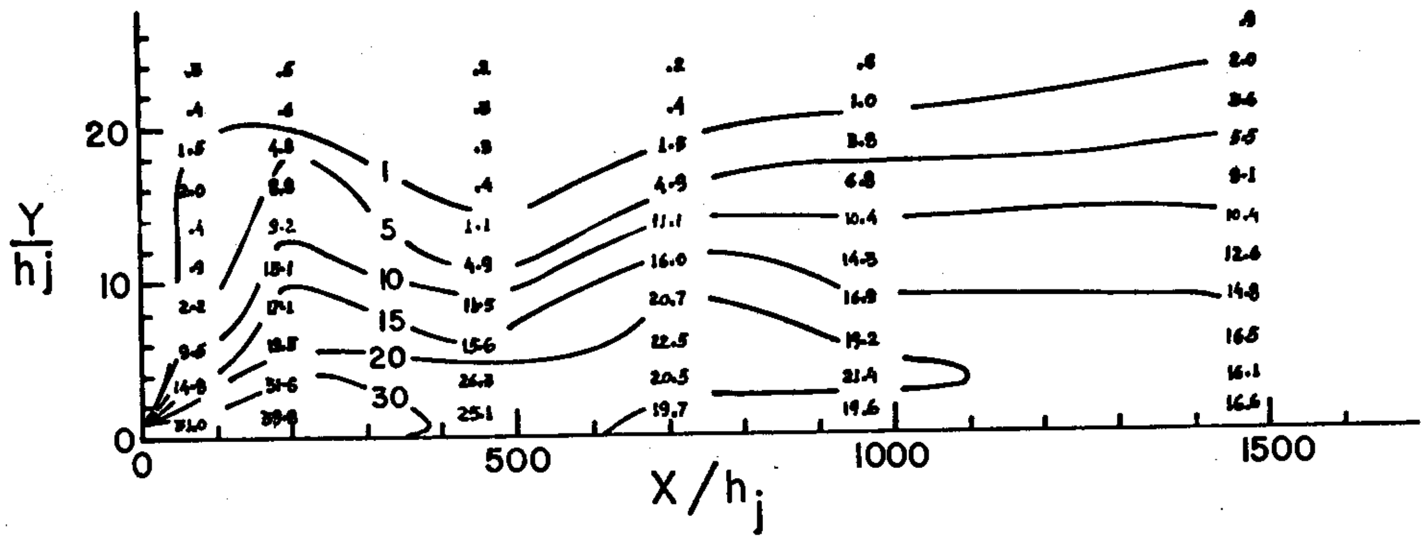

Figure 6c Undistorted Model K = 17

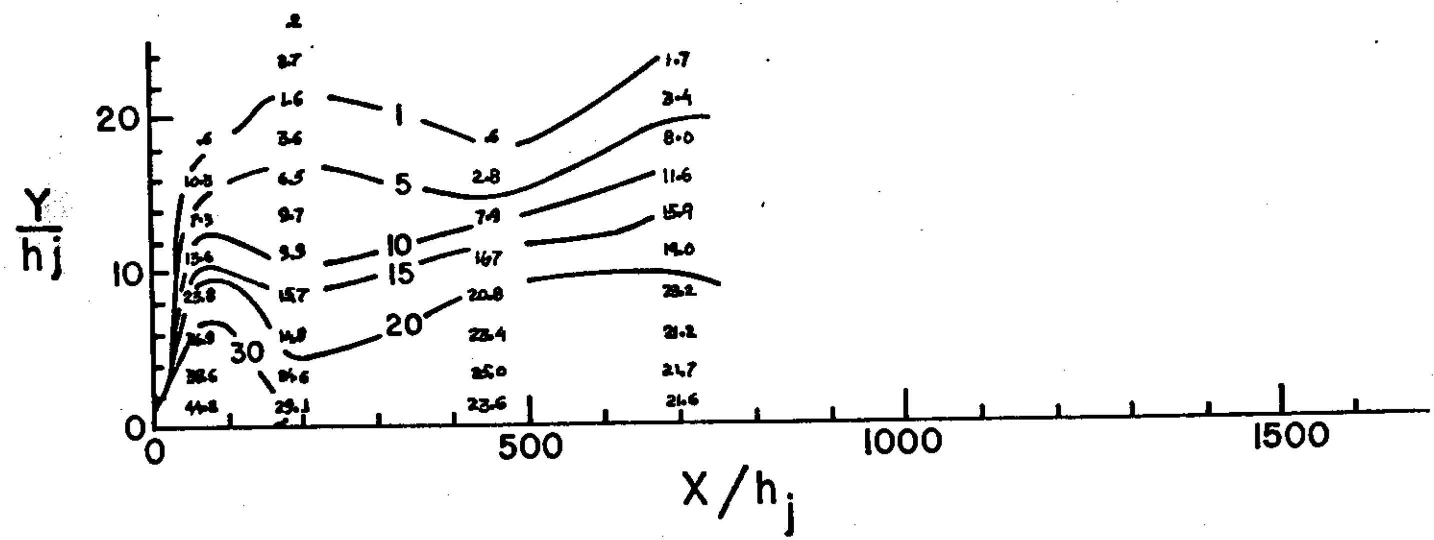

Figure 6d Undistorted Model K = 30

Figure 7 Transverse Temperature Distribution - Distorted Model

RUN NO. D1 $\frac{x}{h_j} = 11$

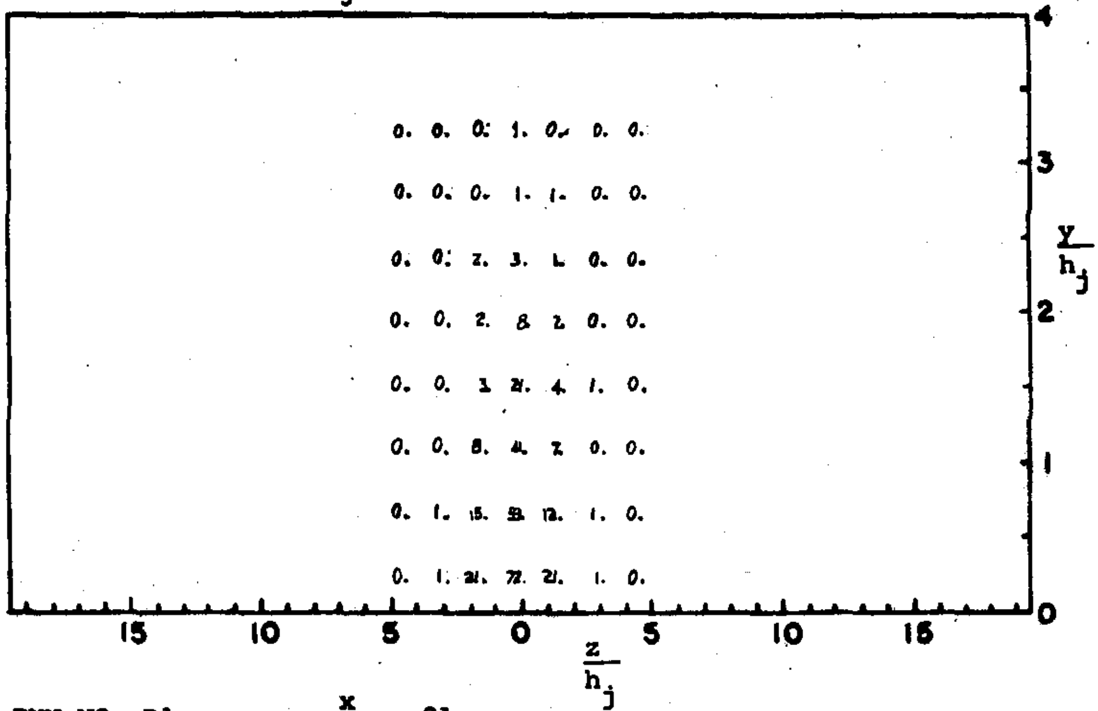

RUN NO. D1 $\frac{x}{h_j} = 21$

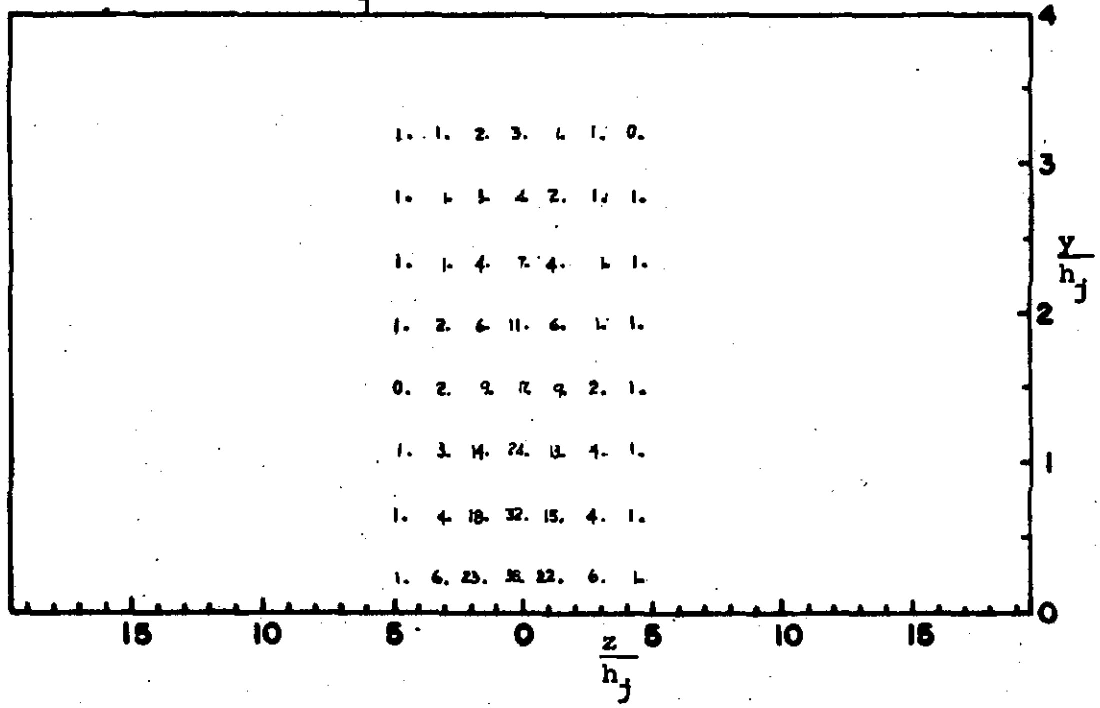

Figure 7a: K = 1

RUN NO. D1 $\frac{x}{h_j} = 43$

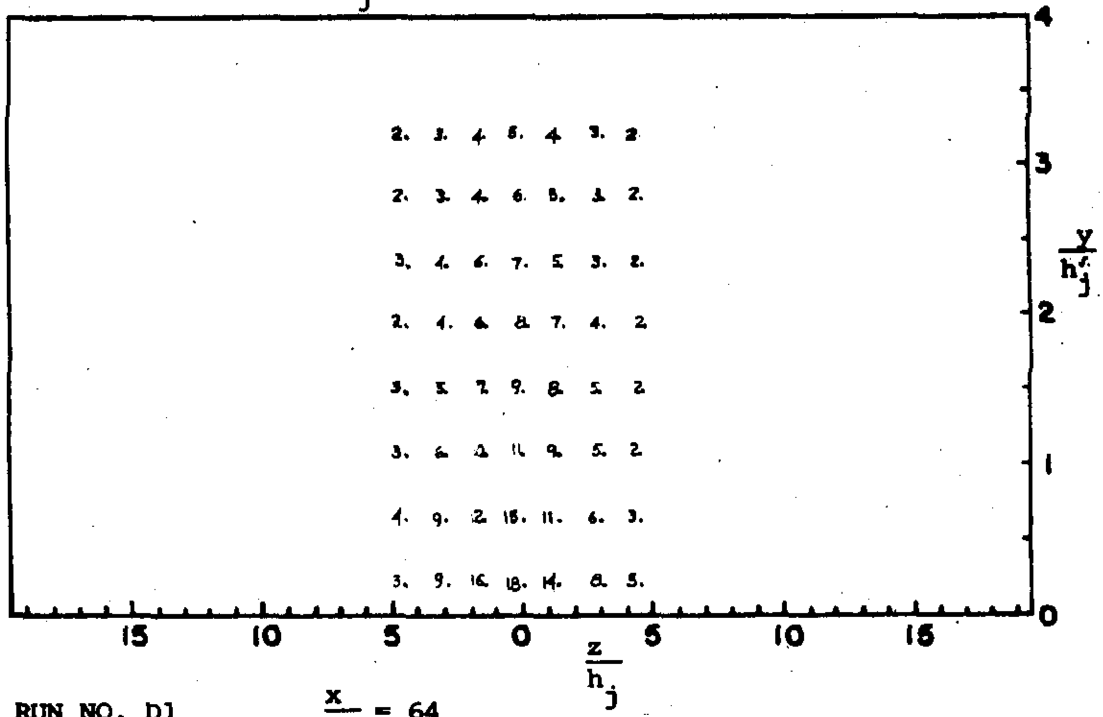

RUN NO. D1 $\frac{x}{h_j} = 64$

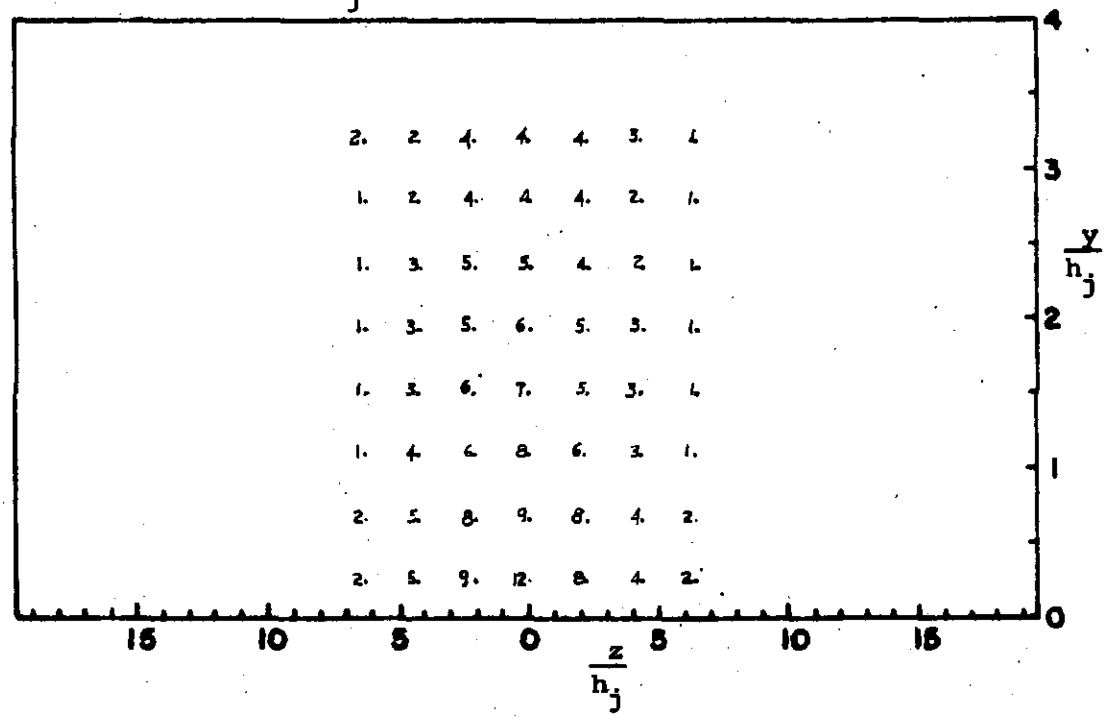

Figure 7a (ctd.) K = 1

RUN NO. D1 $\frac{x}{h_j} = 86$

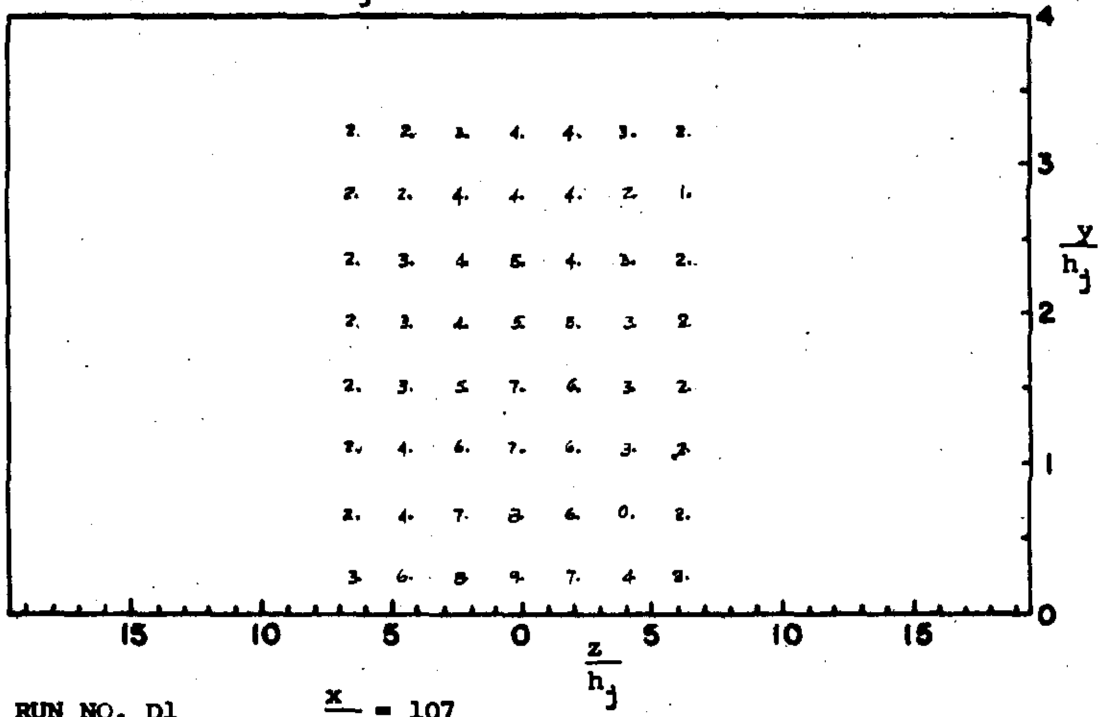

RUN NO. D1 $\frac{x}{h_j} = 107$

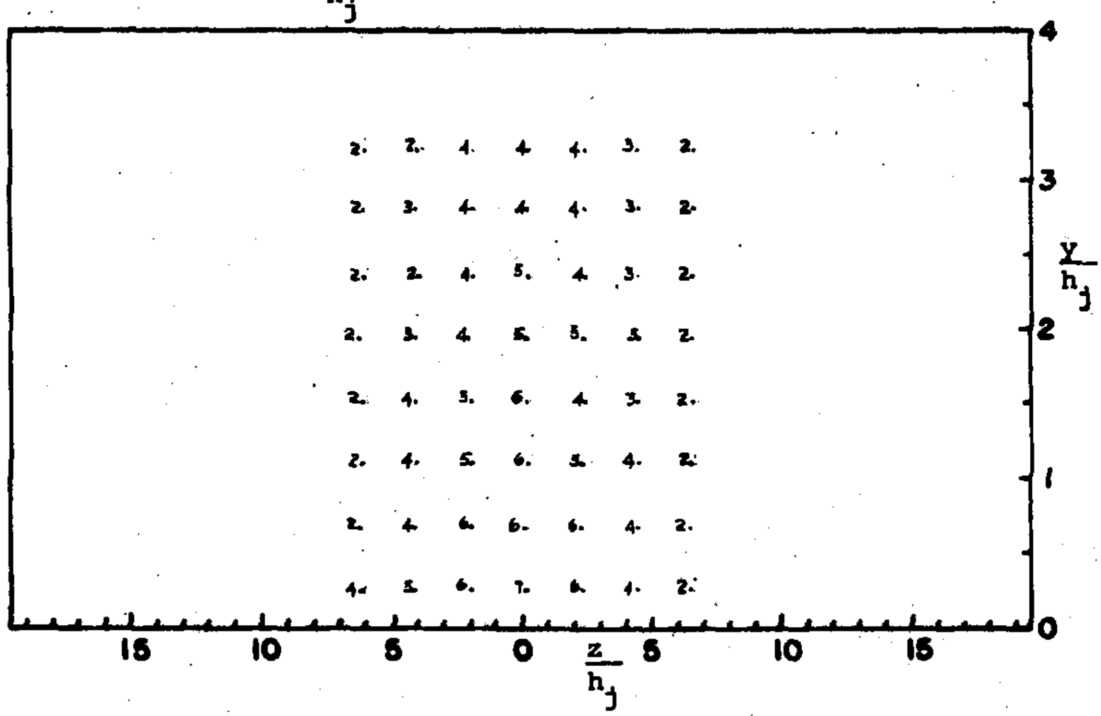

Figure 7a (ctd.) K = 1

RUN NO. D1 $\frac{x}{h_j} = 150$

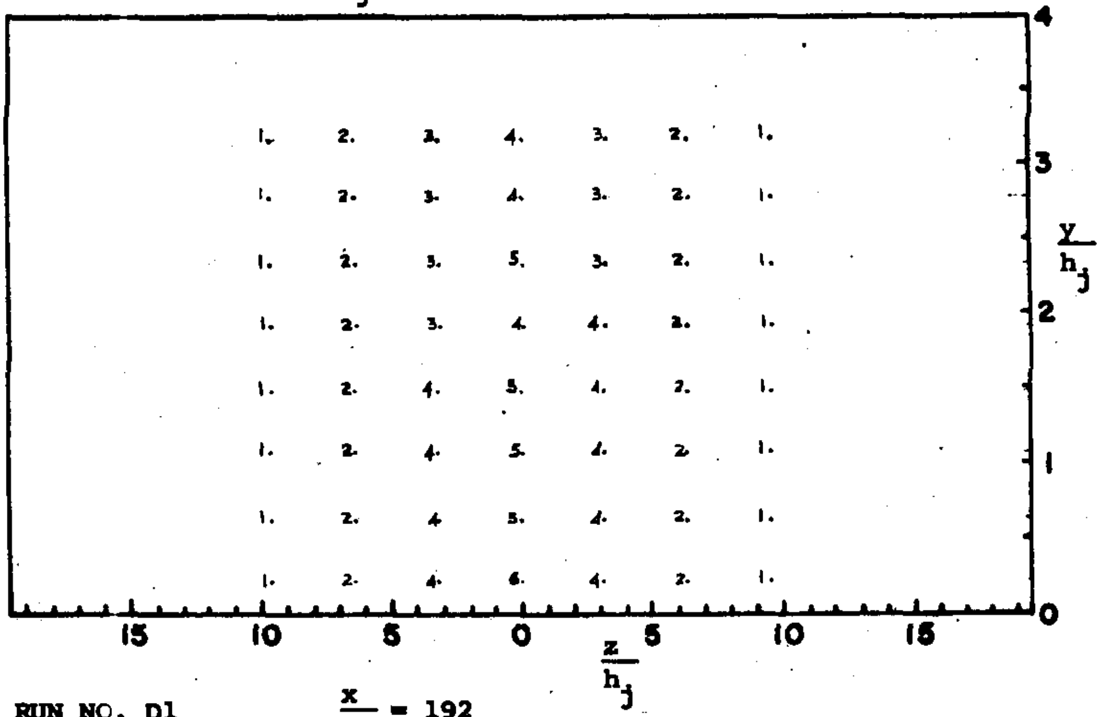

RUN NO. D1 $\frac{x}{h_j} = 192$

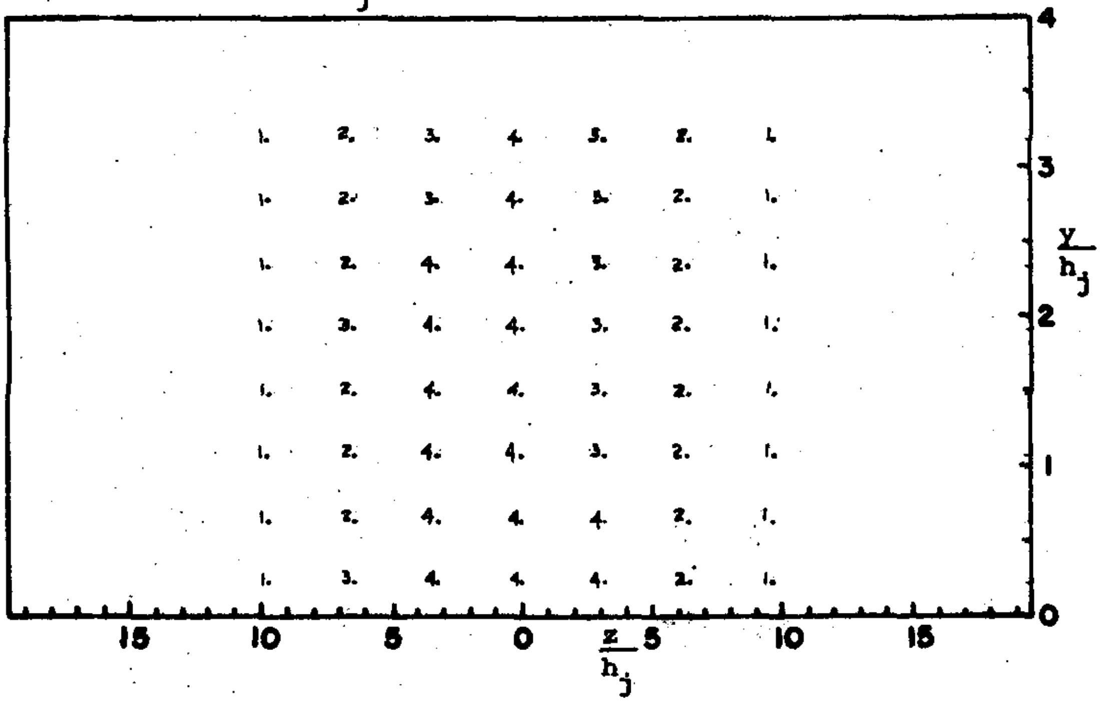

Figure 7a (ctd.) K = 1

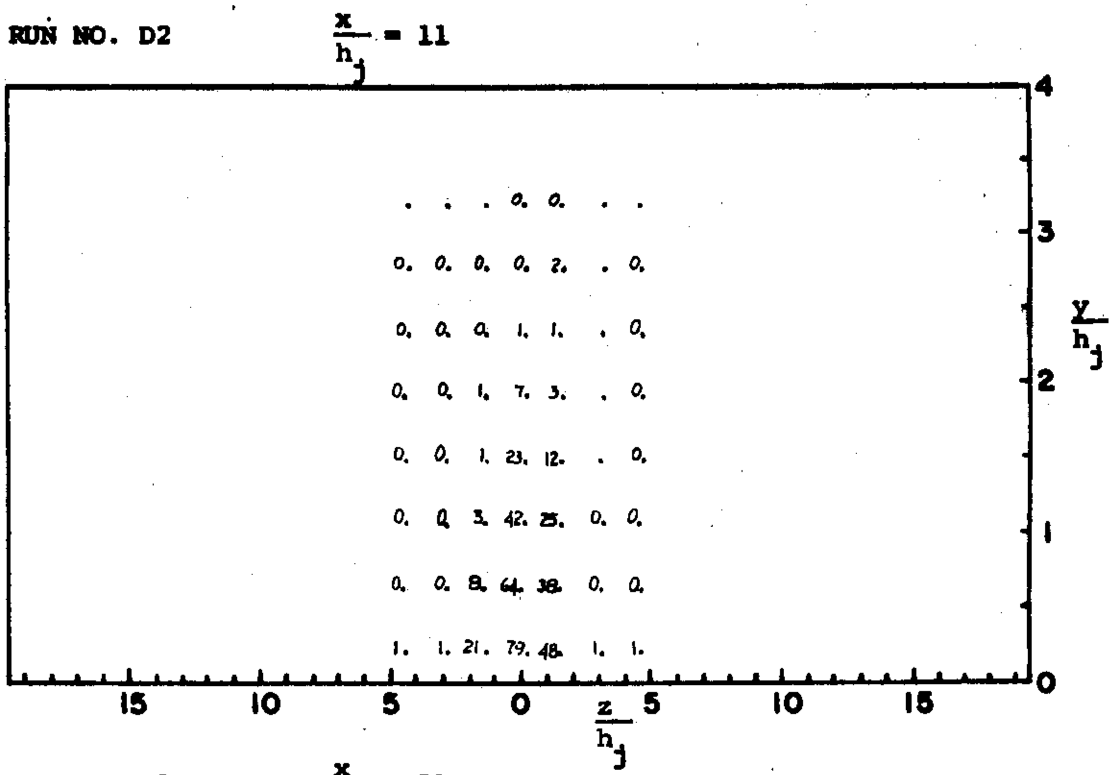

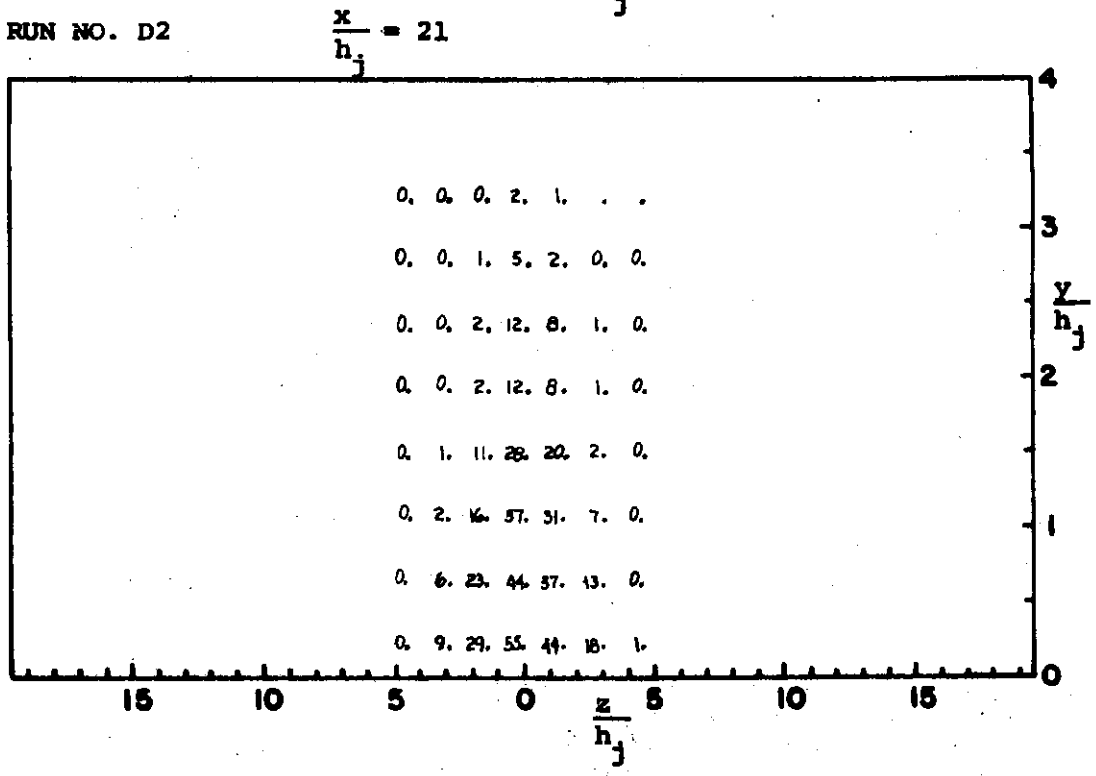

Figure 7b: K = 3.2

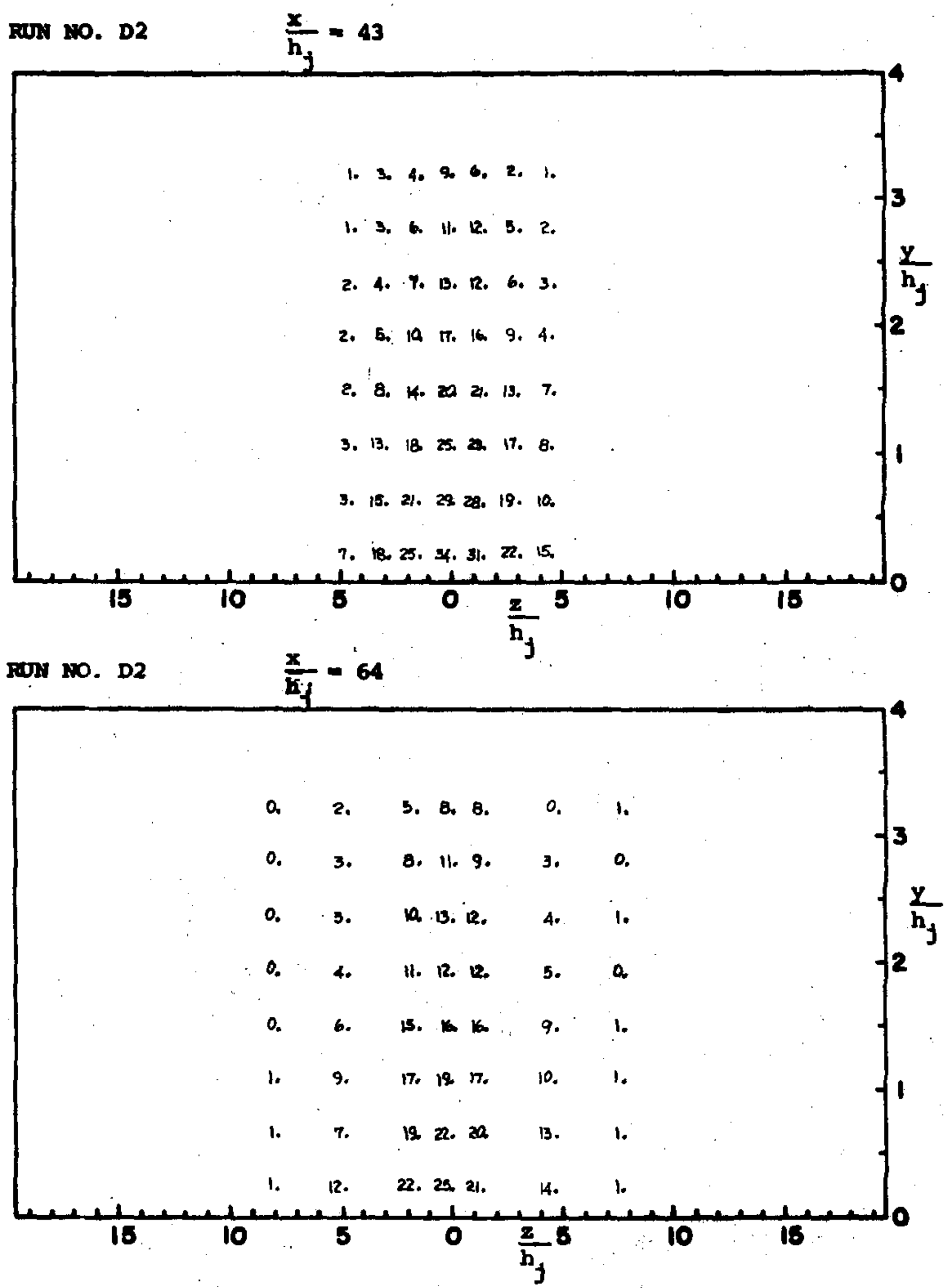

Figure 7b (ctd.) K = 3.2

RUN NO. D2 $\frac{x}{h_j} = 86$

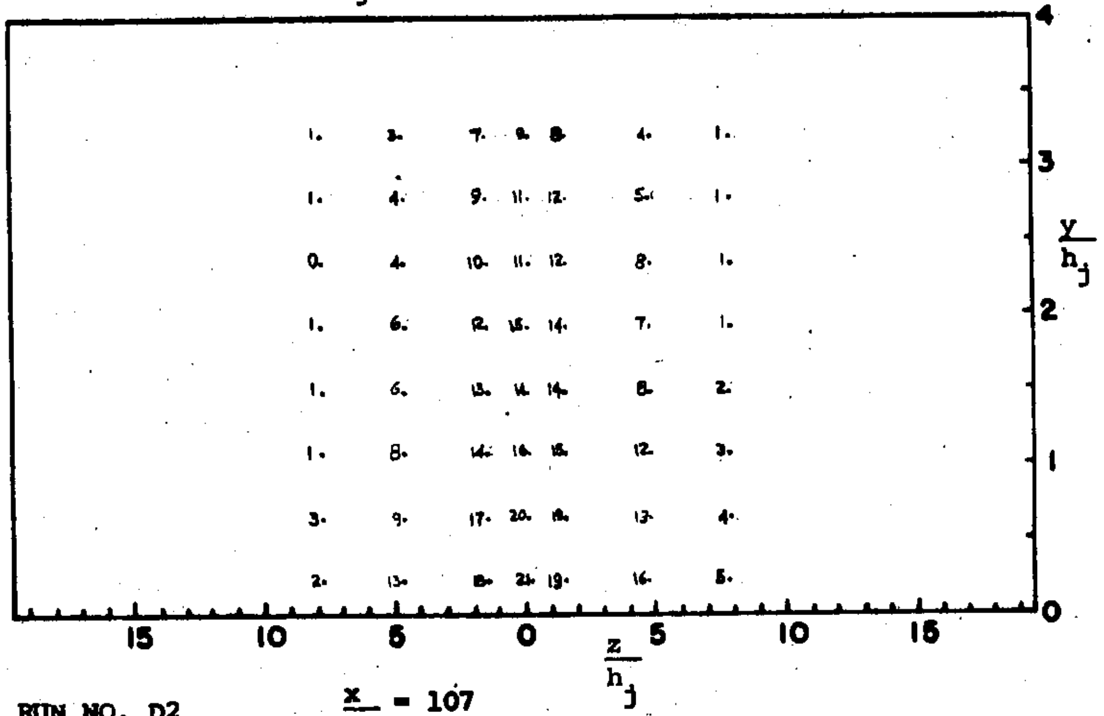

RUN NO. D2 $\frac{x}{h_j} = 107$

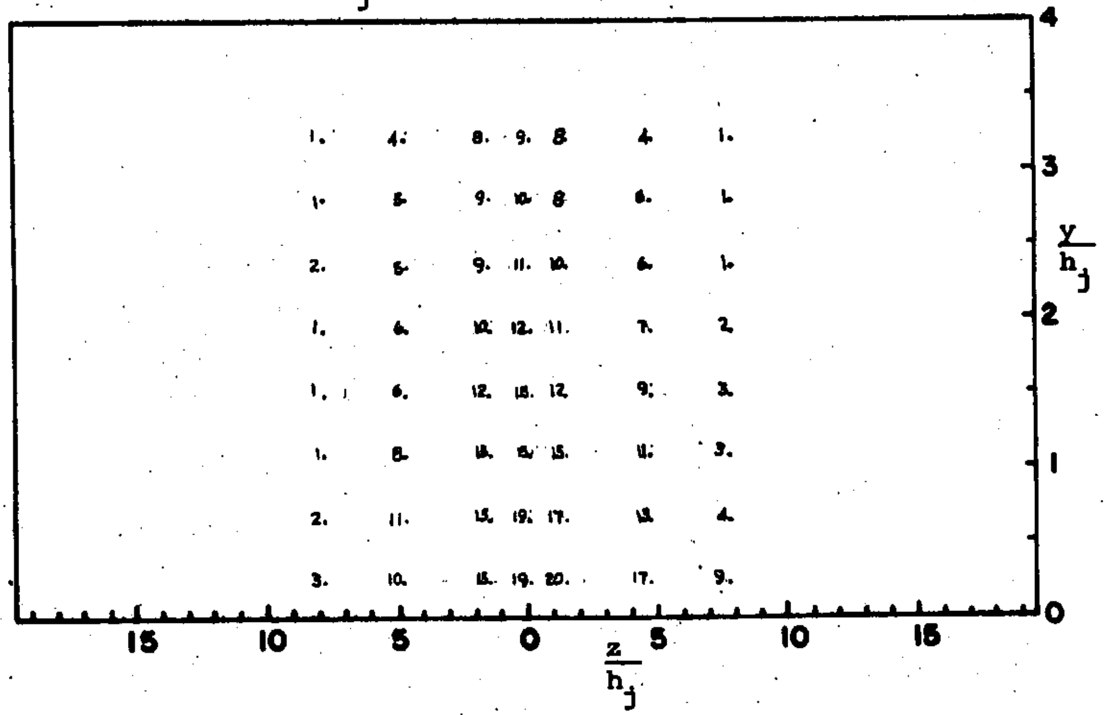

Figure 7b (ctd.) K = 3.2

RUN NO. D2 $\frac{x}{h_j} = 150$

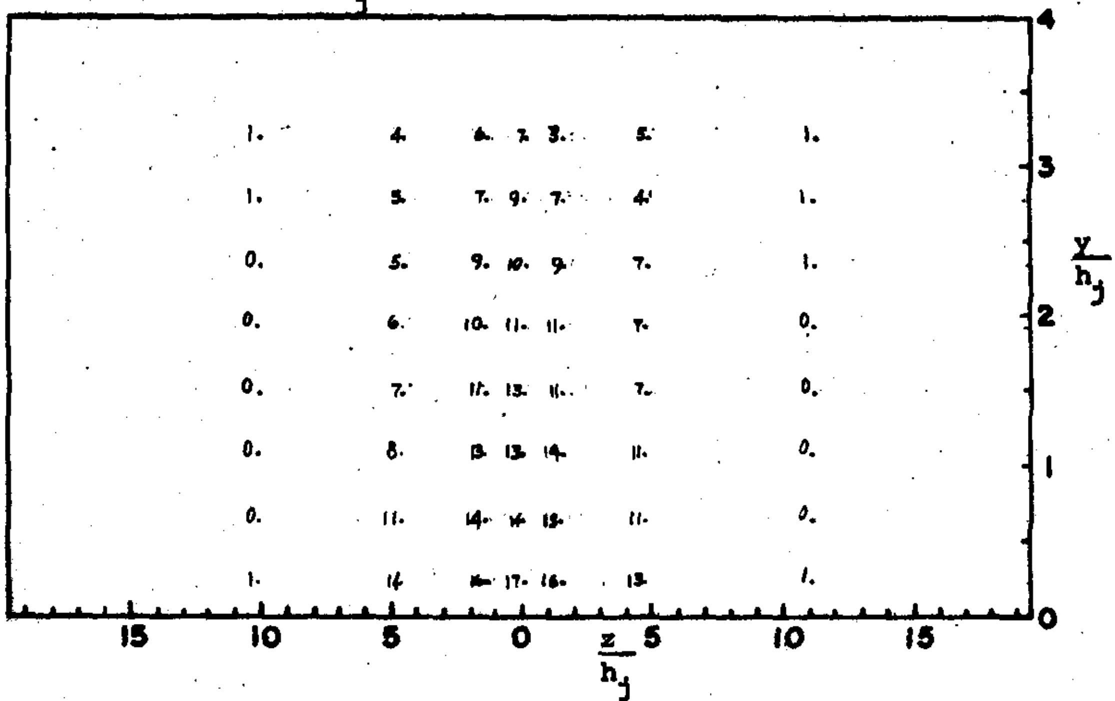

RUN NO. D2 $\frac{x}{h_j} = 192$

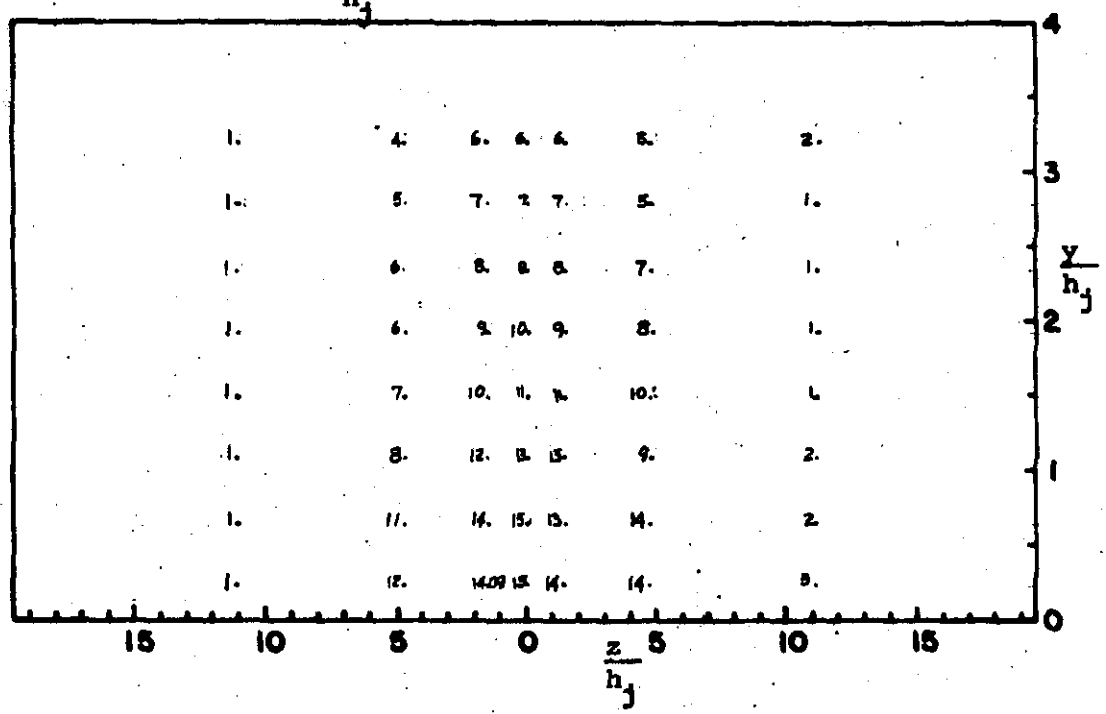

Figure 7b (ctd.) K = 3.2

RUN NO. D3 $\frac{x}{h_j} = 11$

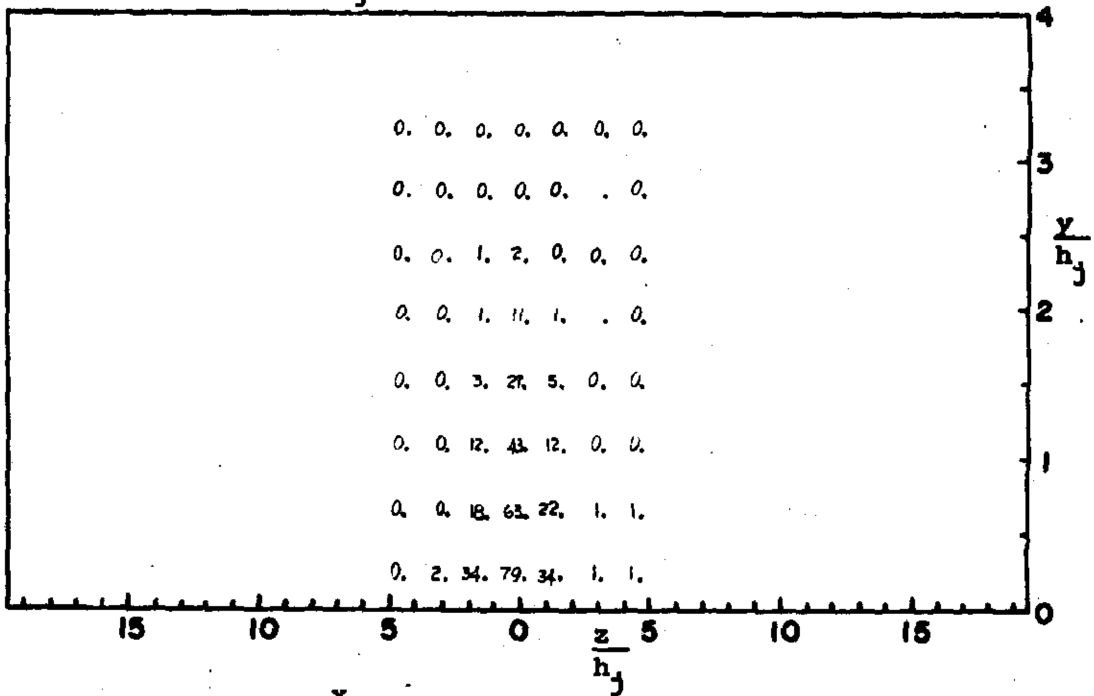

RUN NO. D3 $\frac{x}{h_j} = 21$

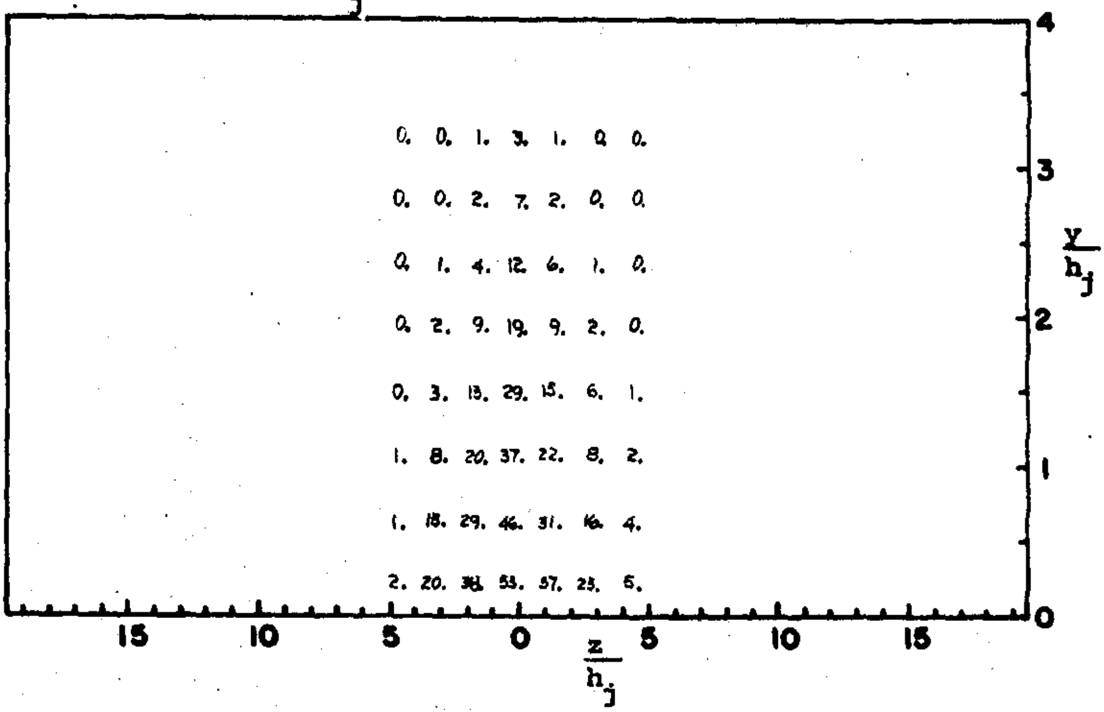

Figure 7c: K = 4.1

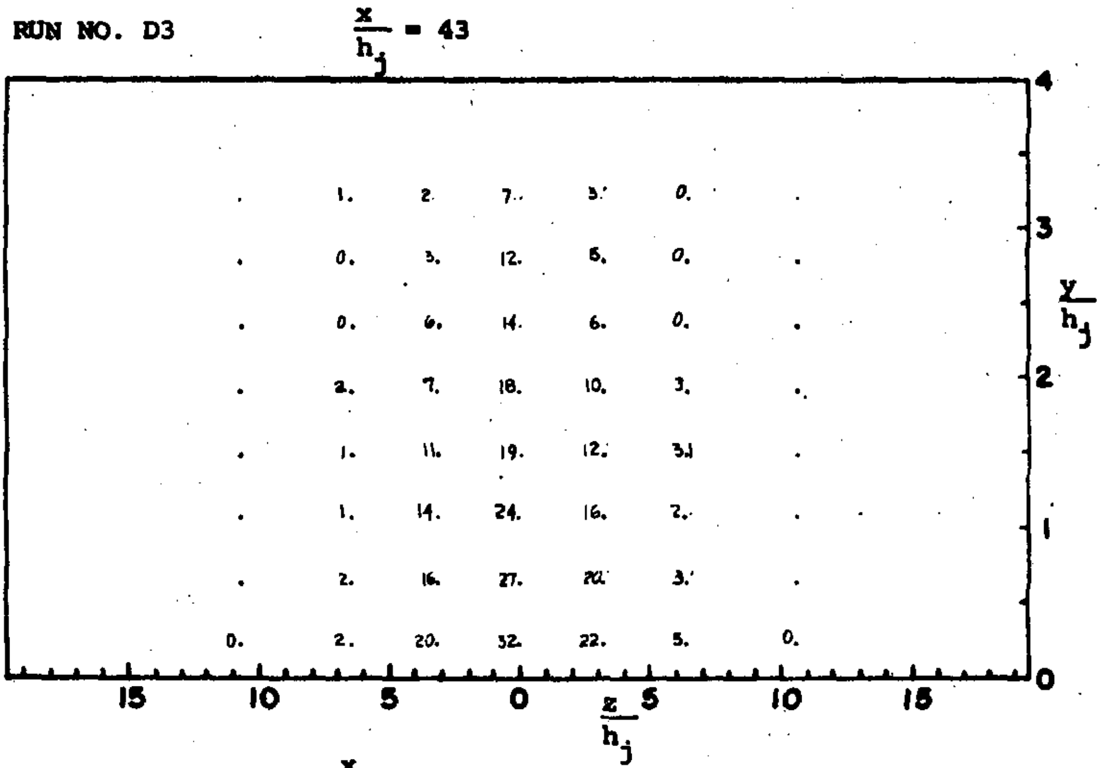

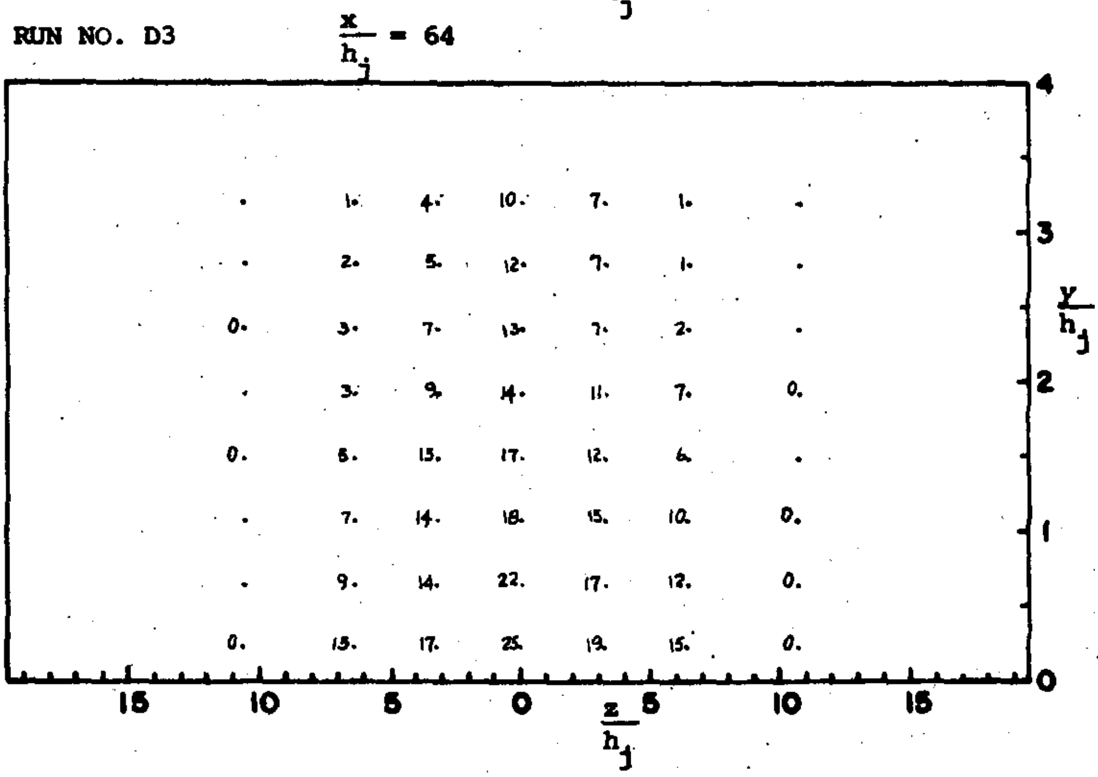

Figure 7c (ctd.) K = 4.1

RUN NO. D3 $\frac{x}{h_j} = 86$

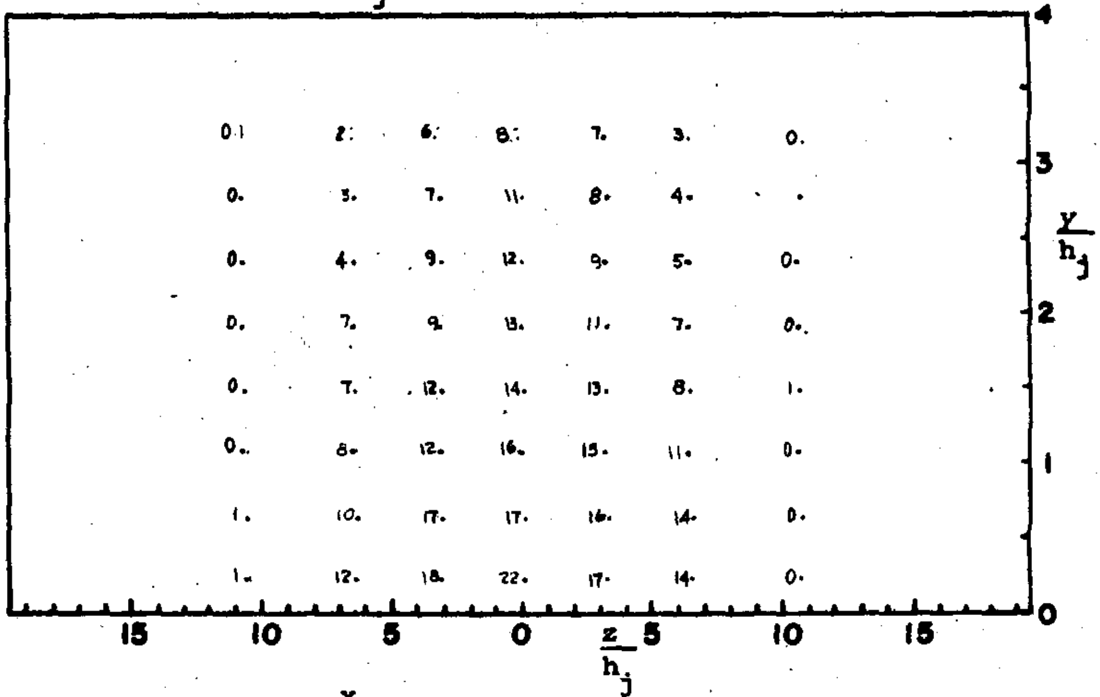

RUN NO. D3 $\frac{x}{h_j} = 107$

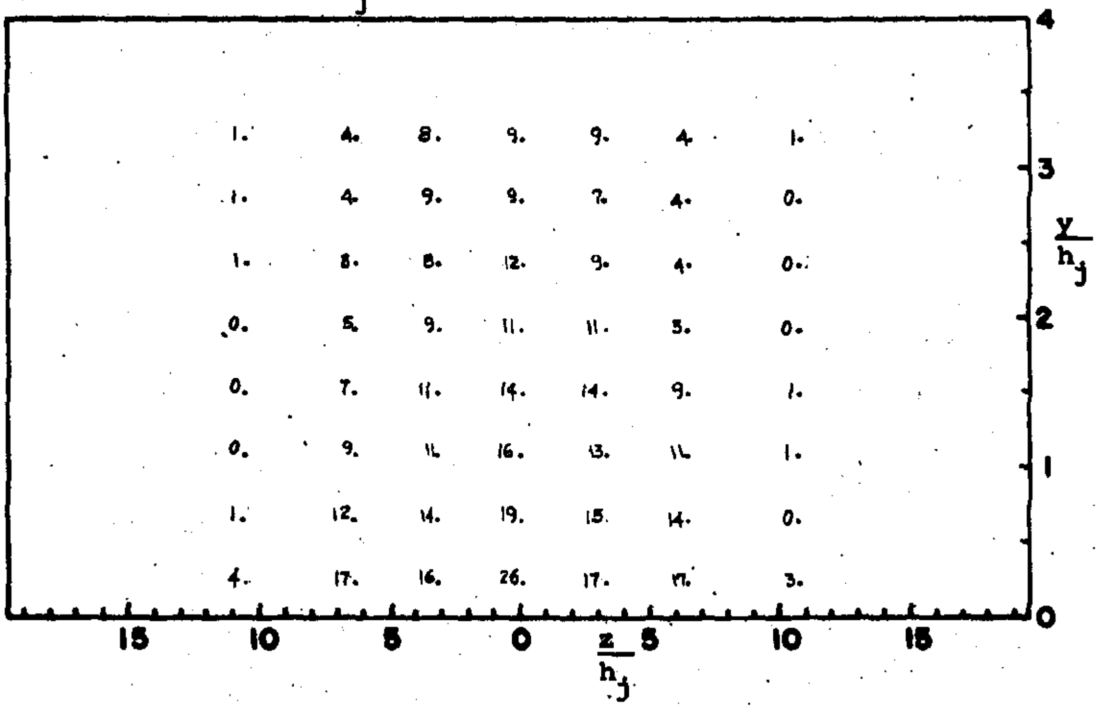

Figure 7c (ctd.) K = 4.1

RUN NO. D3 $\frac{x}{h_j} = 150$

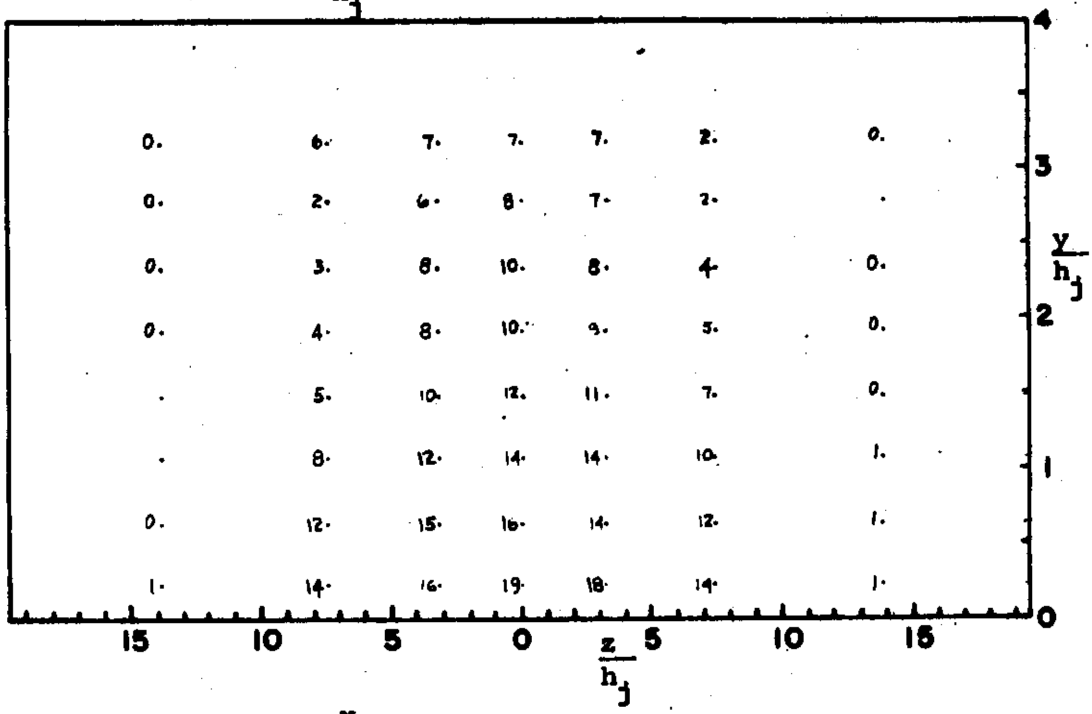

RUN NO. D3 $\frac{x}{h_j} = 192$

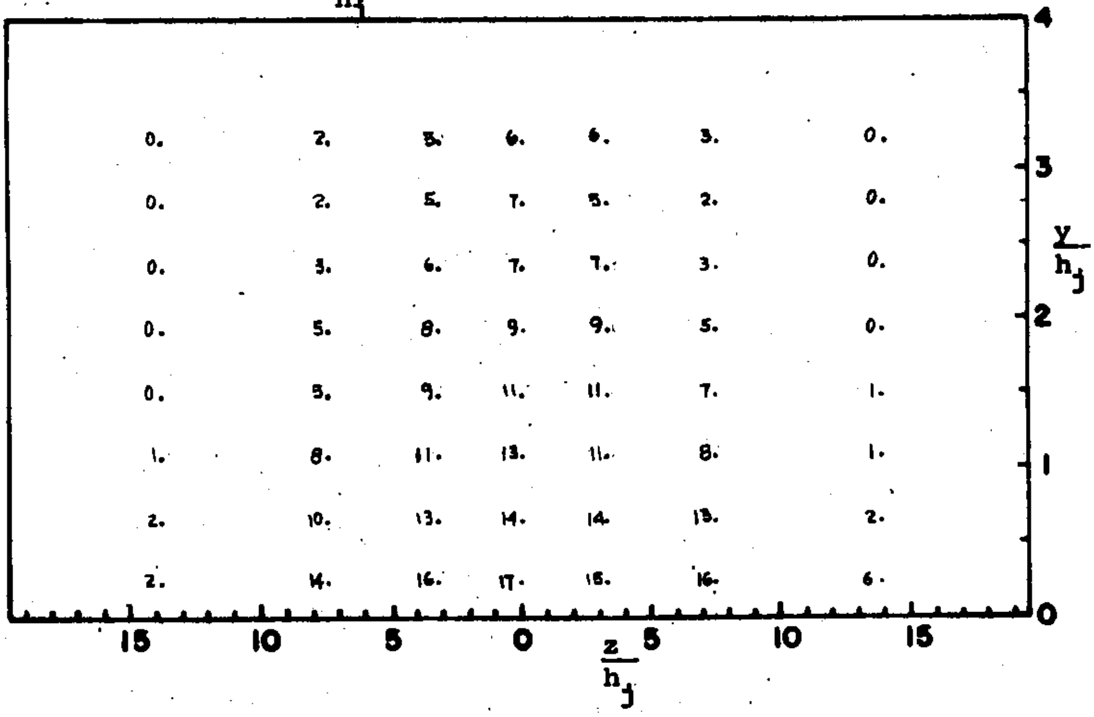

Figure 7c (ctd.) K = 4.1

RUN NO. D4 $\frac{x}{h_j} = 11$

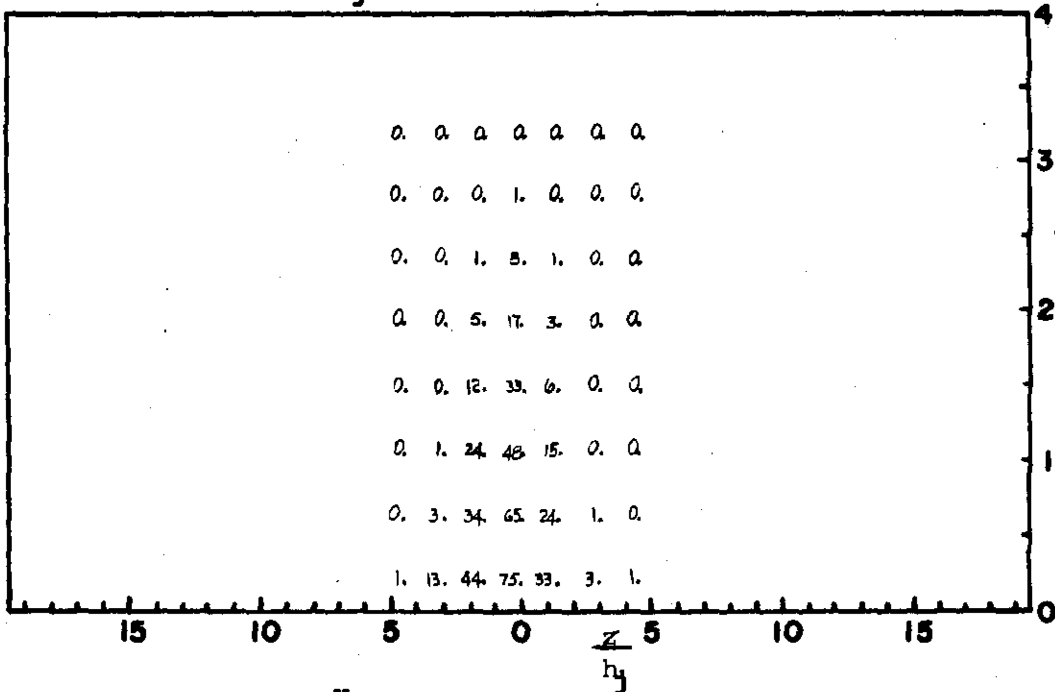

RUN NO. D4 $\frac{x}{h_j} = 21$

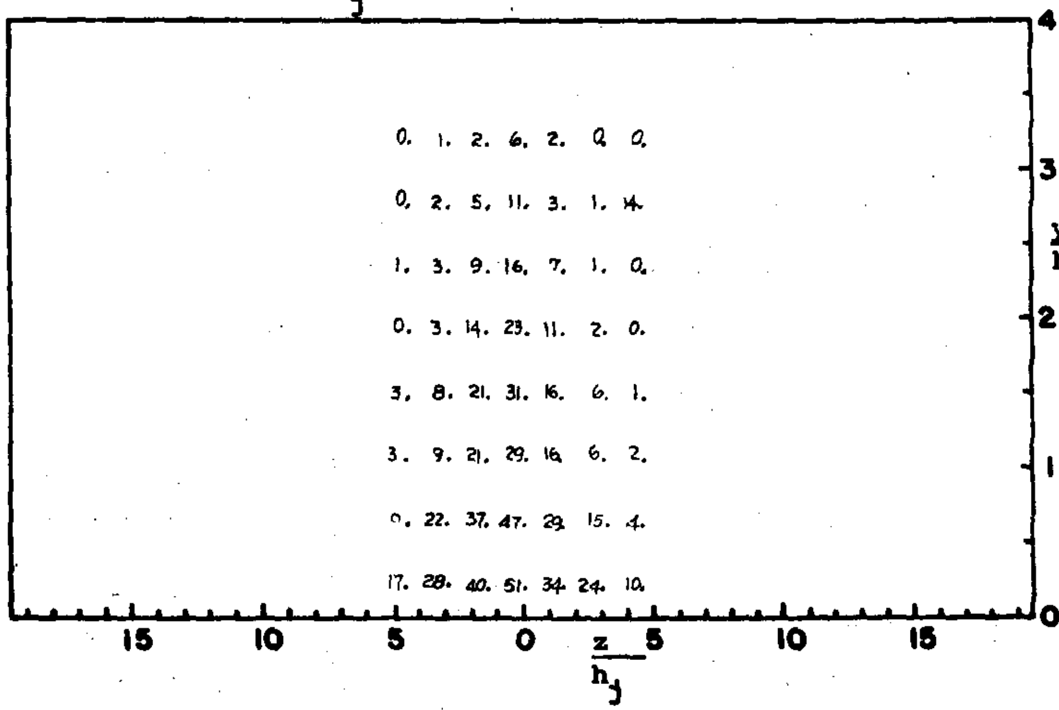

Figure 7d: K = 5

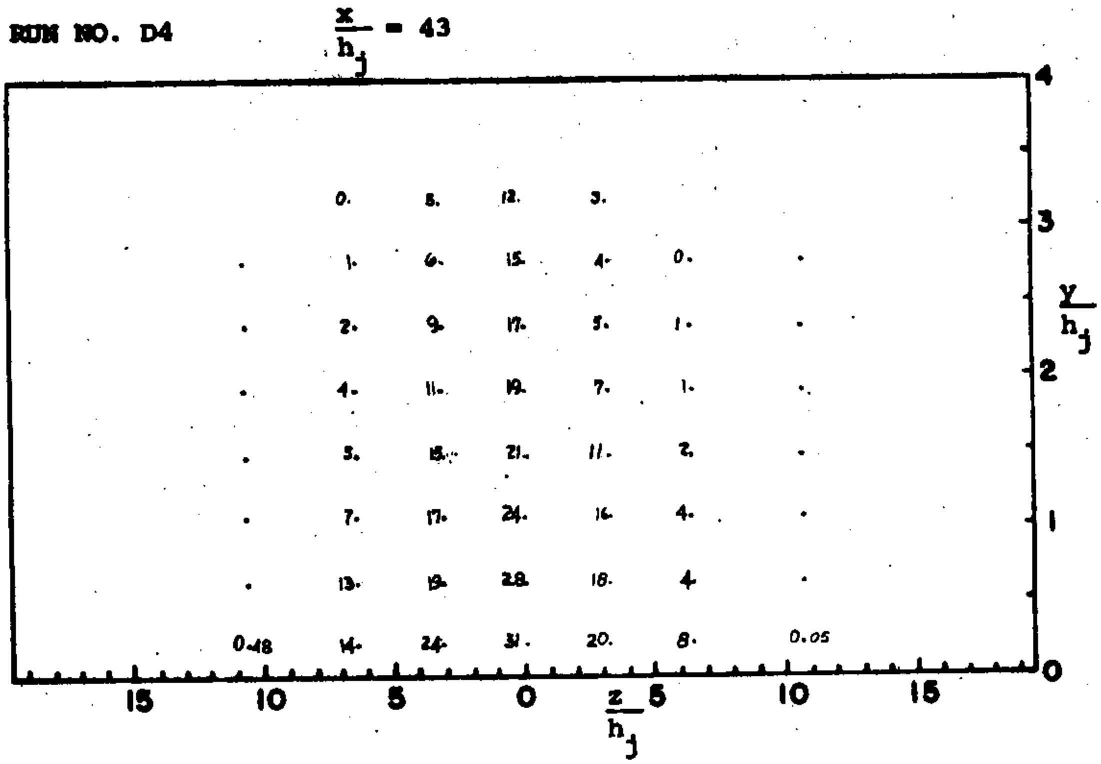

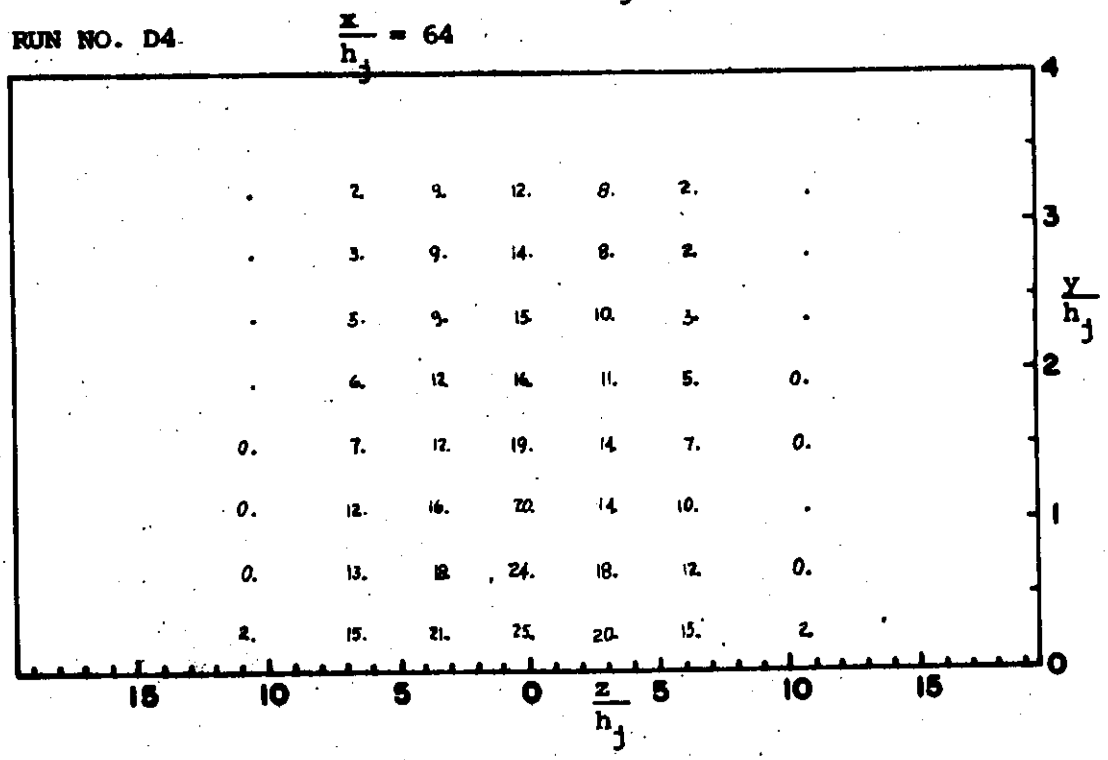

Figure 7d (ctd.) K = 5

RUN NO. D4 $\frac{x}{h_j} = 86$

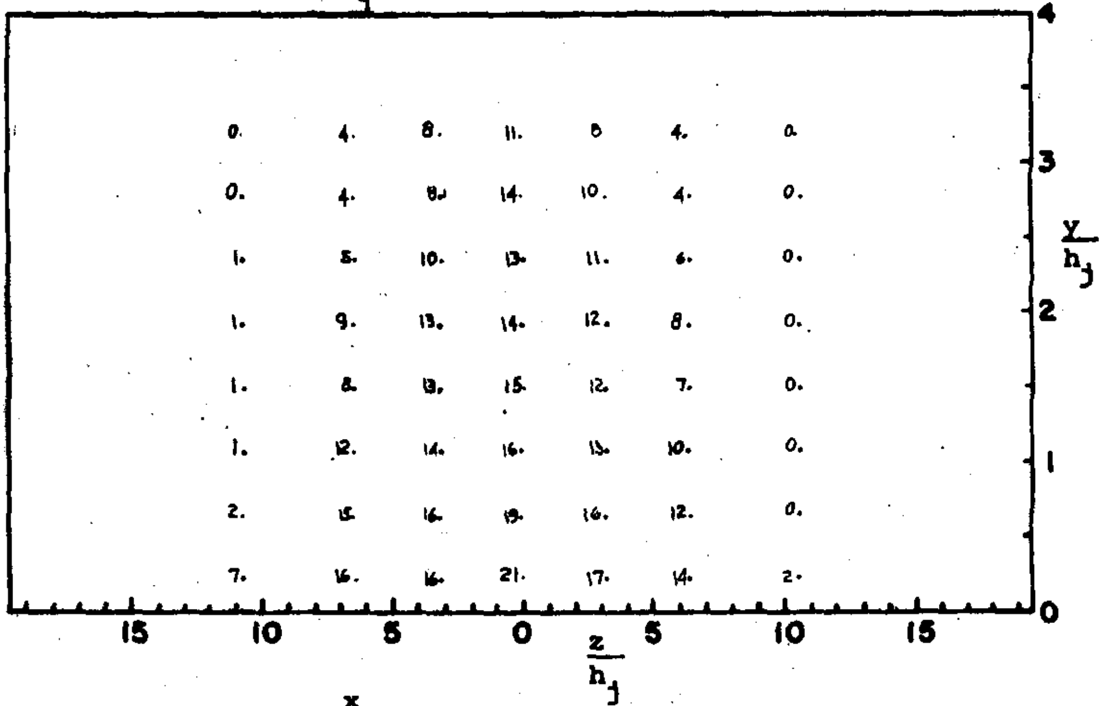

RUN NO. D4 $\frac{x}{h_j} = 107$

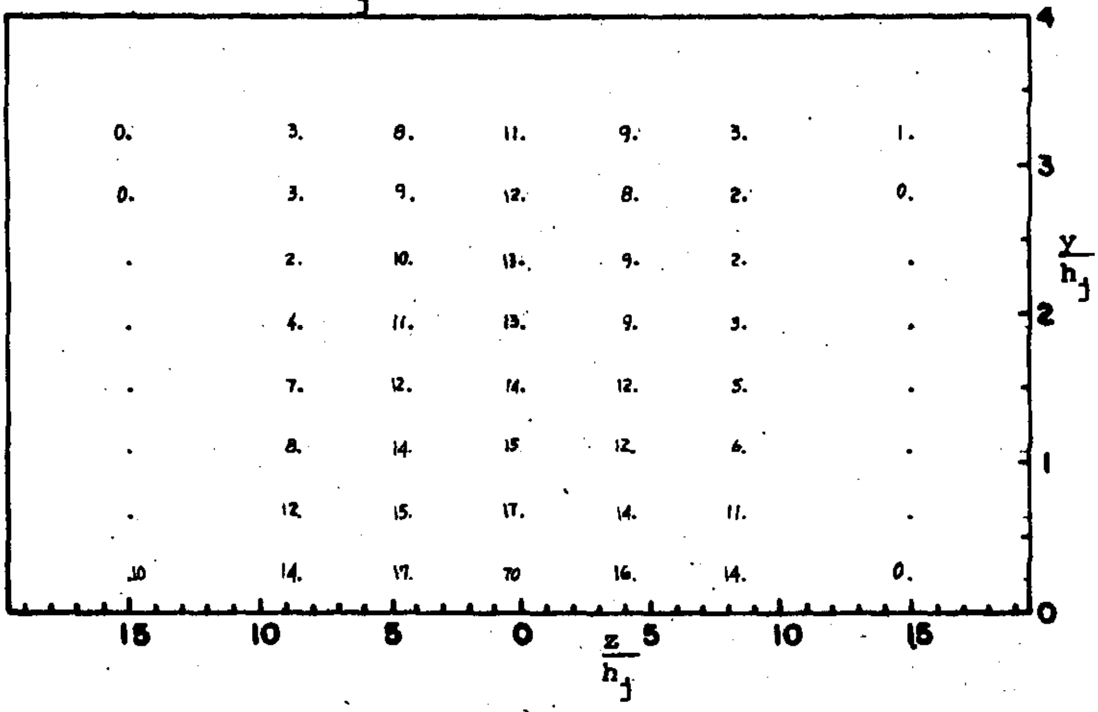

Figure 7d (ctd.) K = 5

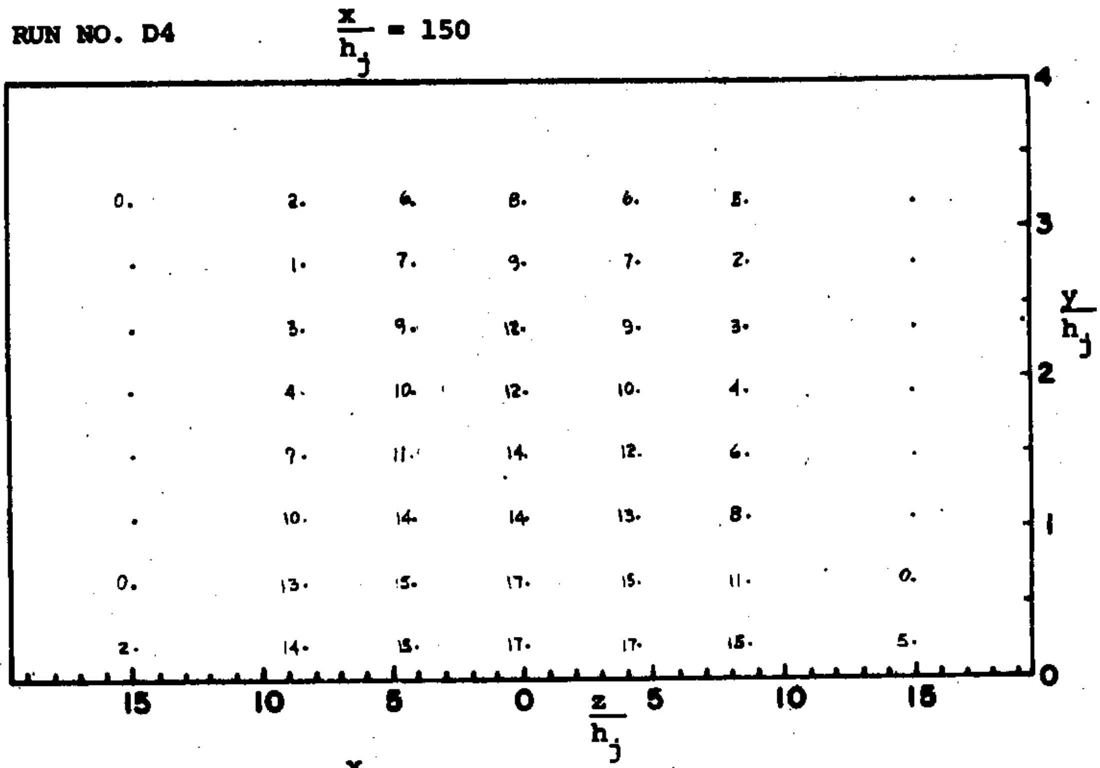

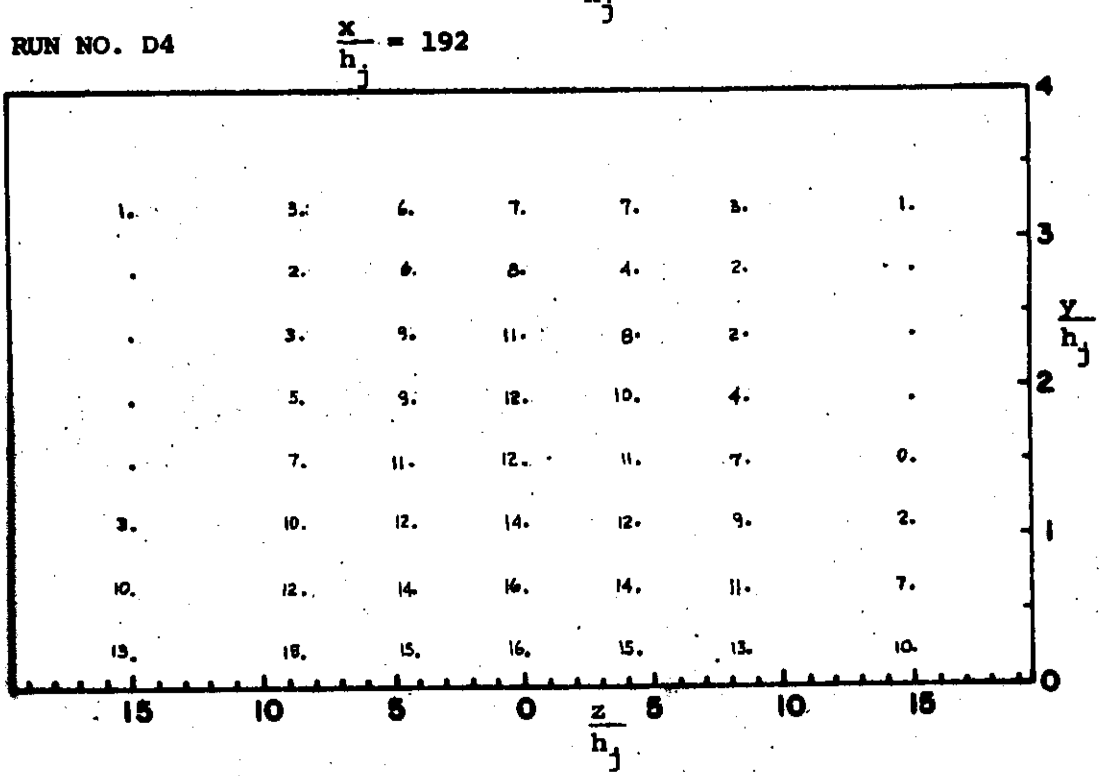

Figure 7d (ctd.) K = 5

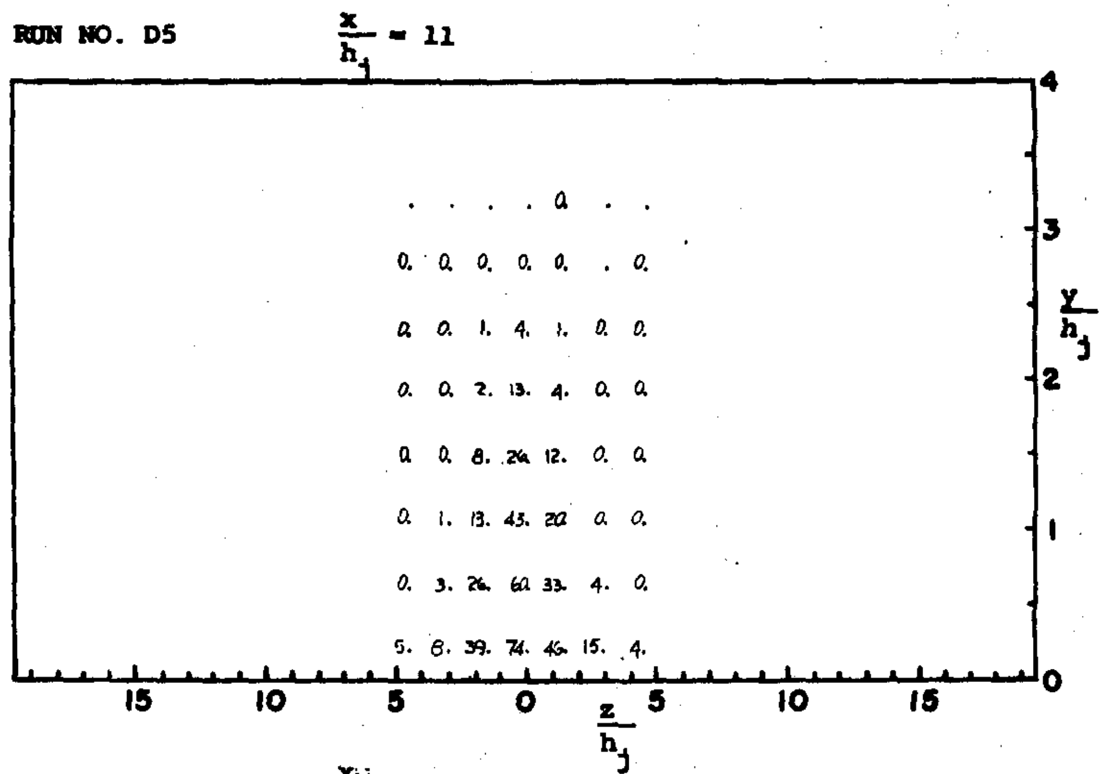

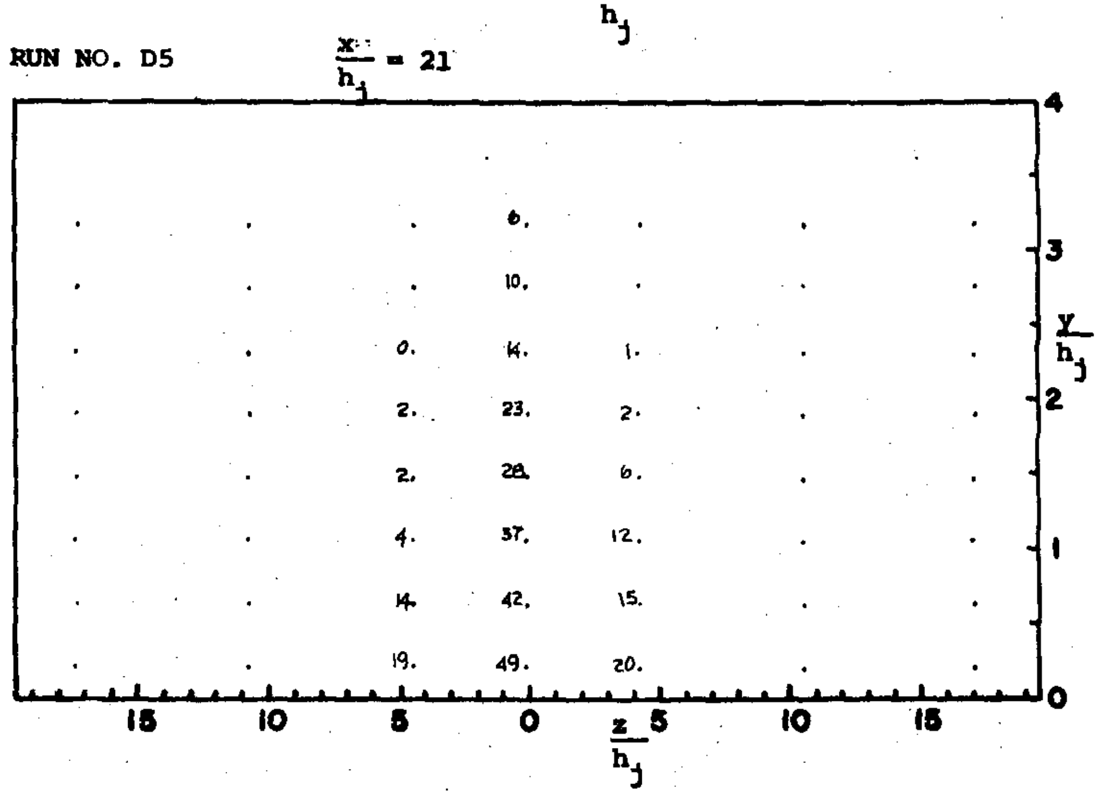

Figure 7e: K = 10

RUN NO. D5 $\frac{x}{h_j} = 43$

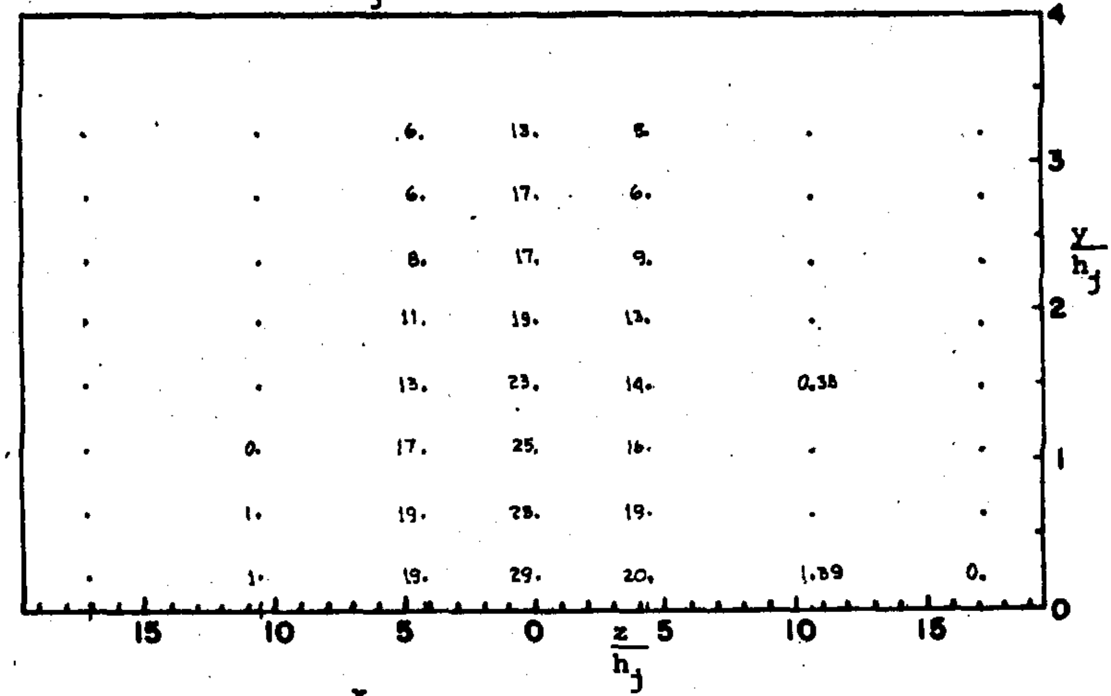

RUN NO. D5 $\frac{x}{h_j} = 64$

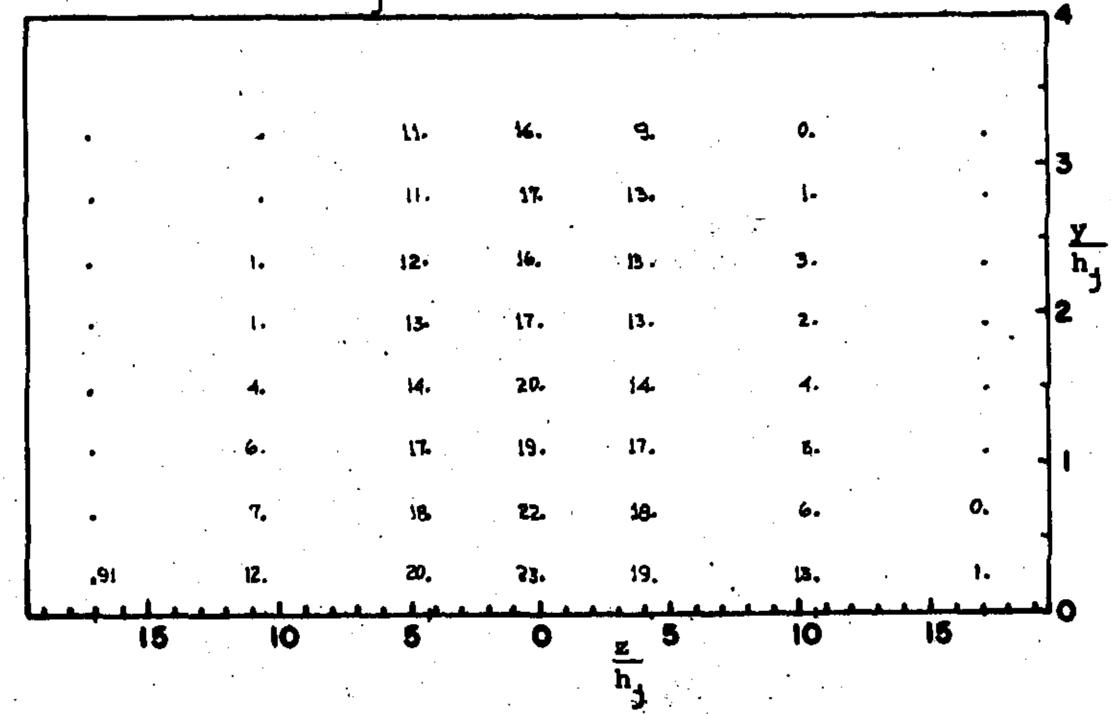

Figure 7e (ctd.) K = 10

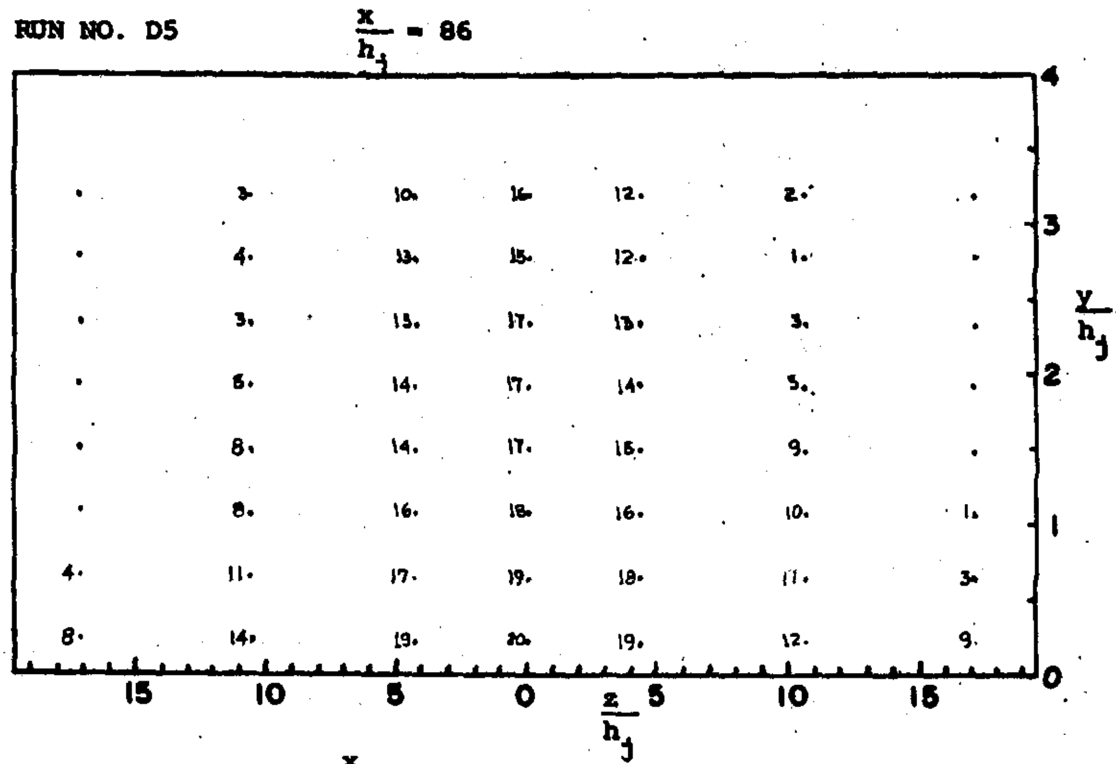

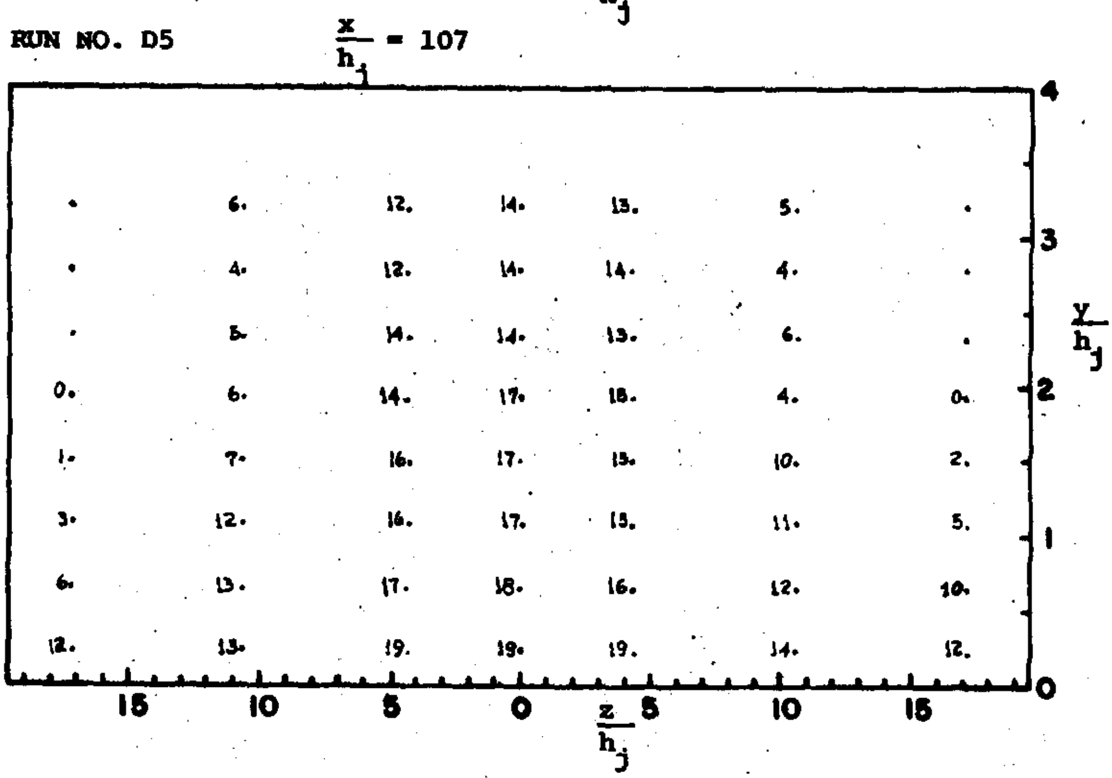

Figure 7e (ctd.) K = 10

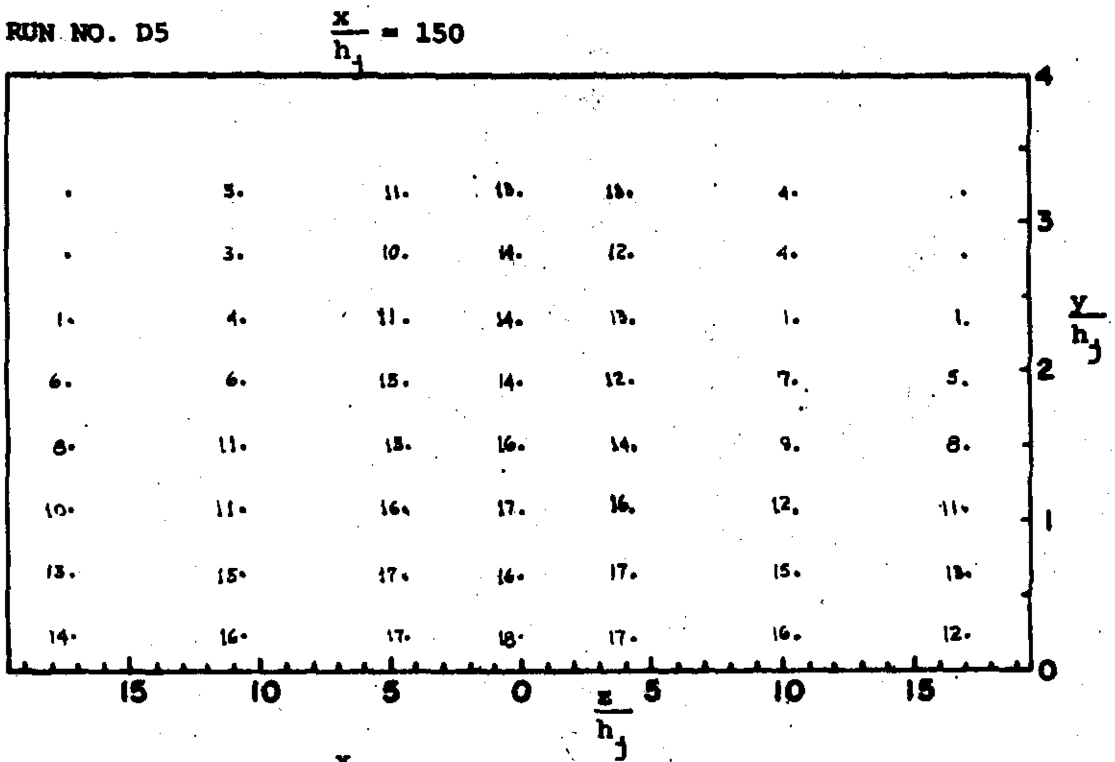

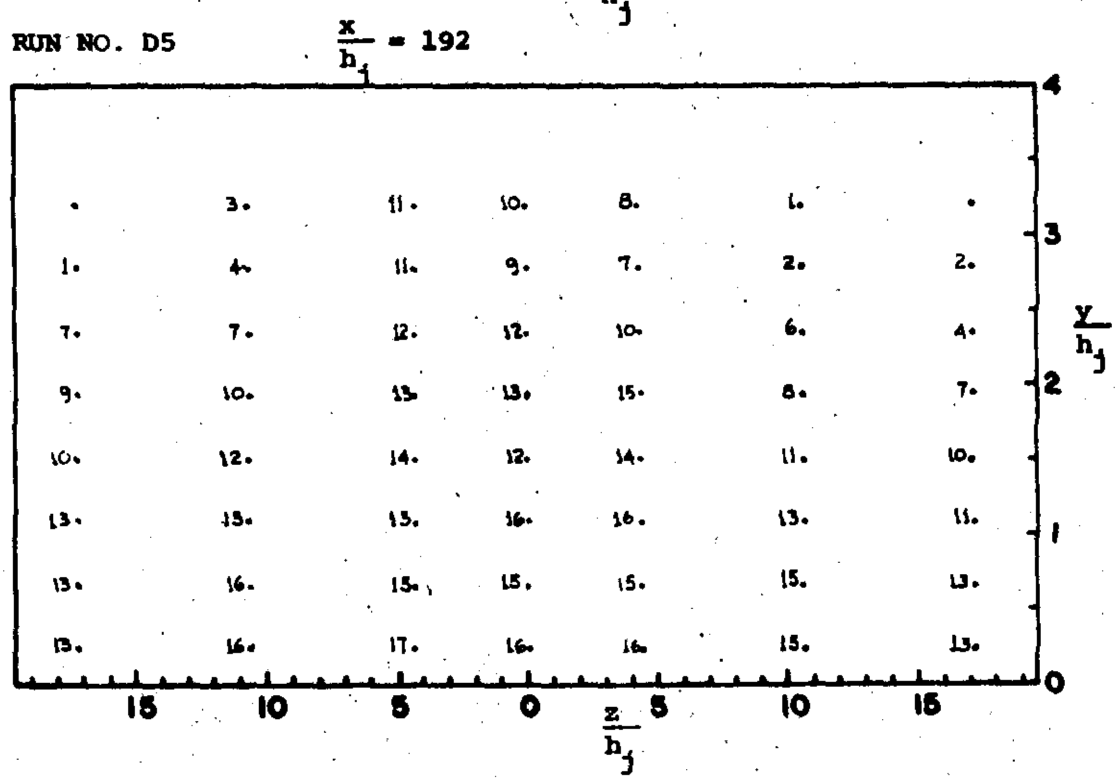

Figure 7e (ctd.) K = 10

Figure 8 Longitudinal Temperature Distribution - Distorted Model

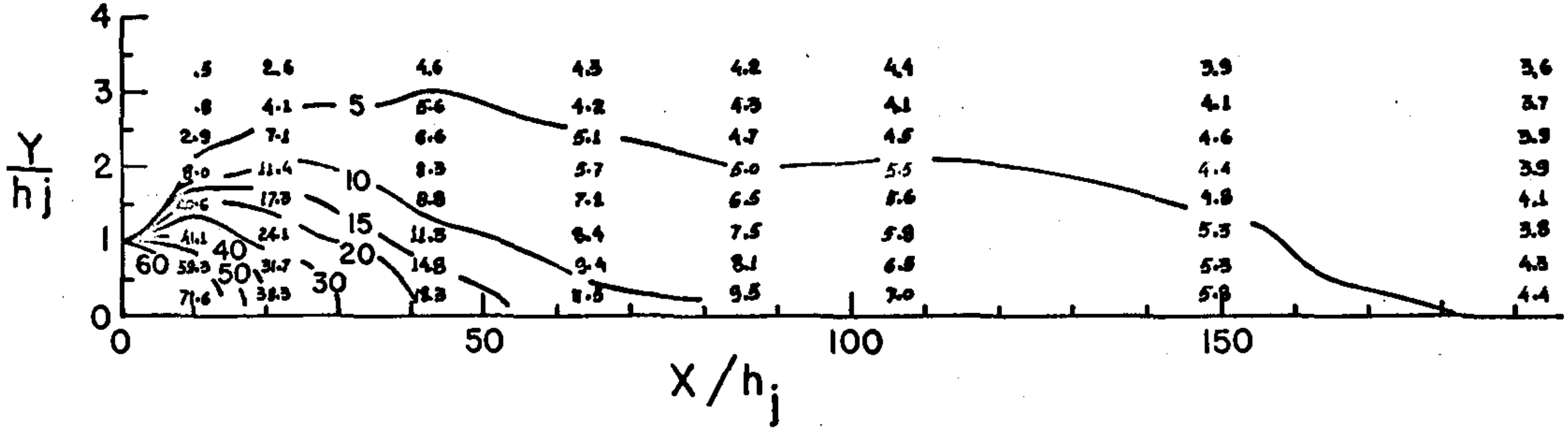

Figure 8a Distorted Model K = 1

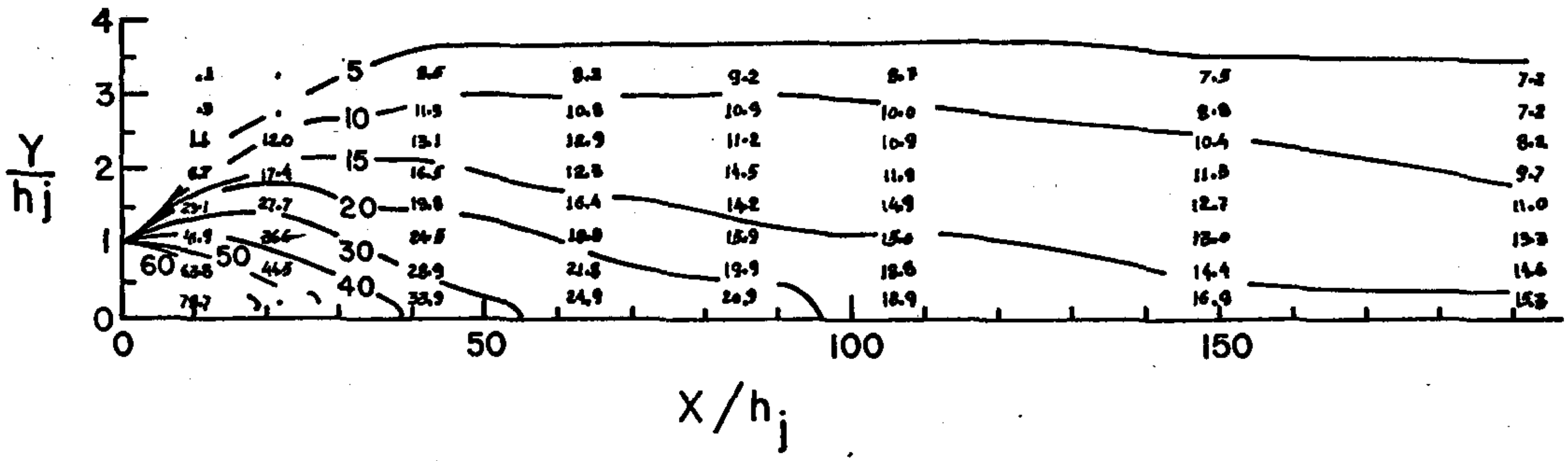

Figure 8b Distorted Model K = 3.2

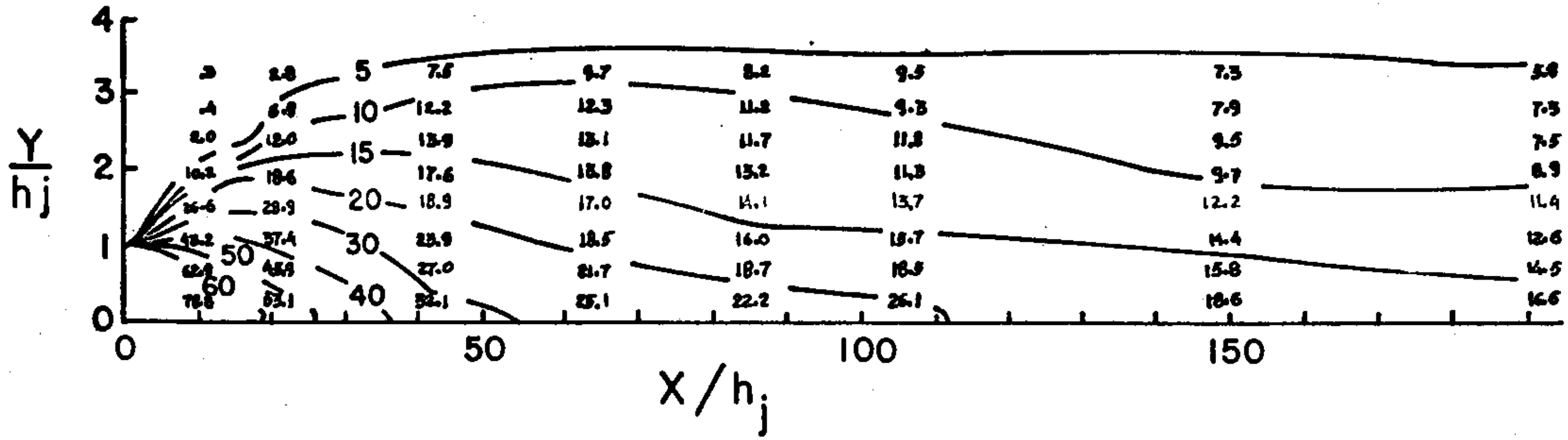

Figure 8c Distorted Model K = 4.1

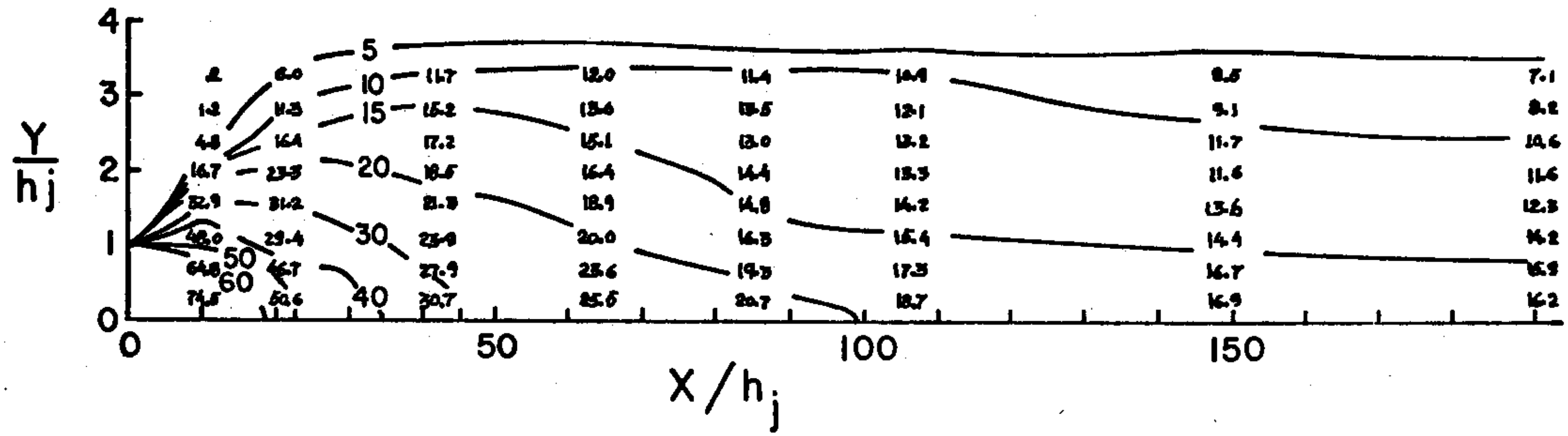

Figure 8d Distorted Model K = 5

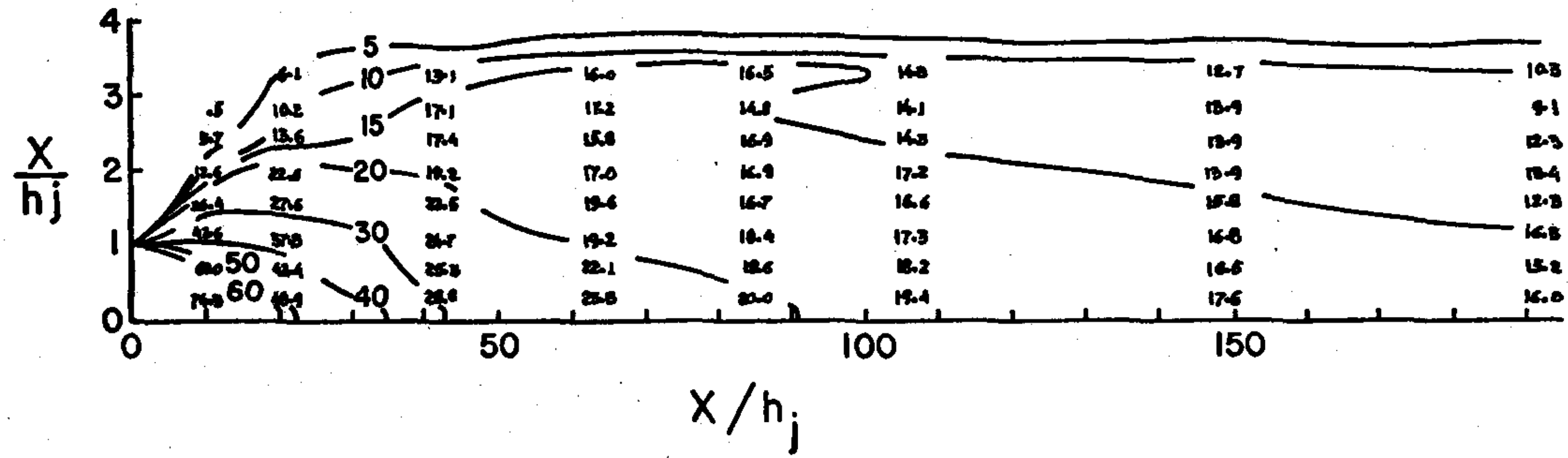

Figure 8e Distorted Model K = 10